



# Modular Solutions for Bridges

## Intermediate Report

31<sup>st</sup> January 2023

Deliverable D4.1



## Technical References

Project acronym	OMICRON
Project full title	'Towards a more automated and optimised maintenance, renewal and upgrade of roads by means of robotised technologies and intelligent decision support tools'
Grant number	955269
Project website	<a href="https://omicronproject.eu/">https://omicronproject.eu/</a>
Coordinator	CEMOSA

Deliverable No.	D4.1
Deliverable nature	R
Work package (WP)	WP4
Task	Task T4.1
Dissemination level <sup>1</sup>	PU
Number of pages	67
Keywords	Hybrid bridge, Overpass, prototype, connection
Due date of deliverable	31 <sup>st</sup> January 2023
Actual submission date	31 <sup>st</sup> January 2023

<sup>1</sup> PU = Public

PP = Restricted to other programme participants (including the Commission Services)

RE = Restricted to a group specified by the consortium (including the Commission Services)

CO = Confidential, only for members of the consortium (including the Commission Services)



## Authors

Name	Beneficiary	Details of contribution
Rita Moura	TDU	Deliverable Author

## Contributors

Name	Beneficiary	Details of contribution
Luis Xavier	ARI	Technical inputs
Pedro Cabral	ARI	Technical inputs
Sara Rabadan	PAV	Official revision
Concepción Toribio Díaz	CEM	Final revision
Jose Solís Hernández	CEM	Final revision

## Document history

V	Date	Beneficiary	Author
V0.1	December 2022	TDU	Rita Moura
V0.2	20 <sup>th</sup> January 2023	TDU	Rita Moura
V0.3	22 <sup>nd</sup> January 2023	TDU	Rita Moura
V0.4	24 <sup>th</sup> January 2023	ARI	Luis Xavier
V0.5	26 <sup>th</sup> January 2023	PAV	Sara Rabadan
V0.6	27 <sup>th</sup> January 2023	ARI	Luis Xavier
R1	31 <sup>th</sup> January 2023	CEM	Concepción Toribio, Jose Solís



## Executive Summary

OMICRON is a European project involving multiple partners from institutions and companies across the continent. It is a multidisciplinary technological endeavour that aims for the development of a platform that intends to enhance the way highway infrastructures are built, maintained and managed.

The objective of this deliverable is to report the current status and developments in the OMICRON project in the context of task T4.1, which is focused on the development of modular solutions for bridges.

The scope of task T4.1 is the design of an enhanced modular and hybrid solution for bridge overpasses. This touches the following key points:

- The optimization of the assets and methods used in bridge construction.
- An increased industrialization of bridge construction by introducing optimized processes in the bridge component production pipeline.
- By focusing on the enhancement of the design of the connection elements between steel and concrete parts of hybrid bridges, significant gains are expected in the robustness, performance and safety of bridge overpasses. The project expects that this will thereby allow a more general use of this type of solution.

The activities comprising task T4.1 are divided into three stages:

1. **Stage 1.** Revision of solutions for hybrid steel and concrete bridges. Development of a monitoring campaign in an already existing bridge.
2. **Stage 2.** Experimental in-lab campaigns on three modular bridge solutions.
3. **Stage 3.** Virtual demonstrator of an enhanced hybrid bridge solution selected from the previous stages.

This deliverable describes and reports the activities and results obtained from the first stage as well as part of the second stage, while the final stage is briefly described.

This report includes an introduction and a set of objectives in sections 1 and 2. It also presents the state-of-the-art and the static and dynamic load tests in sections 3 and 4. The in-lab test description as well as the activities and the results obtained at this stage of the task are presented in sections 5, 6, 7 and 8. The main inputs and results for the next steps are also presented in section 9.

## Disclaimer

This publication reflects only the author's view. The Agency (CINEA) and the European Commission are not responsible for any use that may be made of the information it contains.



## Table of contents

Technical References .....	2
Authors .....	3
Contributors .....	3
Document history .....	3
Executive Summary .....	4
Disclaimer.....	4
<b>1 Introduction .....</b>	<b>11</b>
<b>2 Objectives .....</b>	<b>12</b>
<b>3 Background. Modular solution for pre-manufactured bridges .....</b>	<b>13</b>
<b>4 Static and Dynamic Load Tests .....</b>	<b>17</b>
4.1 Description of the overpass PS35 .....	17
4.2 Numerical model.....	19
4.3 Static Load Tests.....	20
4.4 Dynamic tests.....	27
4.5 Load test conclusions .....	37
<b>5 Enhanced Bridge Modular Solution .....</b>	<b>39</b>
5.1 Prototype definition.....	39
5.2 Applied loads.....	41
<b>6 Design and performance of In-lab tests at LNEC .....</b>	<b>43</b>
6.1 Objectives.....	43
6.2 Description of the tests.....	43
6.3 Laboratory conditions .....	44
6.4 Fabrication, transport and installation .....	46
6.5 Prototype instrumentation .....	47
6.6 Expected results .....	49
<b>7 Prototype (scaled model) production.....</b>	<b>52</b>
7.1 Prototype reinforced concrete part production .....	52
7.2 Prototype steel structure production .....	54
7.3 Prototype transportation to LNEC facilities .....	58
<b>8 In-lab tests .....</b>	<b>60</b>
8.1 Instrumentation .....	60
8.2 Laboratory tests .....	61
8.3 Preliminary results .....	62
<b>9 Conclusions and next steps.....</b>	<b>66</b>



9.1 Conclusions .....	66
9.2 Next steps .....	66
<b>10 References .....</b>	<b>67</b>



## Table of tables

Table 1. Weights and lengths of the trucks.....	20
Table 2. Vertical displacements (mm).....	24
Table 3. Longitudinal rotations (arc seconds) .....	24
Table 4. Dynamic test setups (T-transverse direction; V-vertical direction).....	27
Table 5. Identified vibration modes .....	30
Table 6. Modal components of the transverse vibration modes .....	32
Table 7. Modal components of the vertical and torsional vibration modes.....	32
Table 8. Loads to apply and load effects at the connection.....	42
Table 9. Predicted vertical deflection (mm) at position of load application.....	50
Table 10. Predicted longitudinal rotation (arc seconds) at position of load application .....	50
Table 11. Criteria for the evaluation of prototype configurations.....	51
Table 12. Summary table with some preliminary results for the rotations at the connection (LNEC) .	64



## Table of figures

Figure 1. Steel Structure .....	12
Figure 2. Steel-Concrete girders. Bottom view. ....	13
Figure 3. Steel-Concrete girders. Side view.....	14
Figure 4. Examples of Precast Concrete girders .....	14
Figure 5. Hybrid Bridge.....	14
Figure 6. A Hybrid Bridge. Side and Bottom views.....	15
Figure 7. Widening the main highway (A3, Portugal) .....	15
Figure 8. Precast concrete girders and pre-assembled steel span.....	15
Figure 9. Construction procedure – 1 (Precast segments and steel structure assembly).....	16
Figure 10. Construction procedure – 2 (Concrete slab and final demolition of existing structure) .....	16
Figure 11. Connection element between the steel and concrete parts (Armando Rito, 2012).....	16
Figure 12. PS35 location .....	17
Figure 13. Elevation view of the overpass PS35.....	18
Figure 14. Bottom view of the overpass .....	18
Figure 15. Overpass Cross-sections (Armando Rito, 2012) .....	19
Figure 16. Connection between the steel girders and the precast beams (Armando Rito, 2012) .....	19
Figure 17. Perspective of Finite element model (3D Beam) .....	19
Figure 18. Geometric definition of the trucks .....	20
Figure 19. Load cases considered in the tests.....	21
Figure 20. Trucks at the mid span (Load case 1) .....	21
Figure 21. Trucks at the adjacent mid span (Load case 4) .....	21
Figure 22. Linear position measuring transducer.....	22
Figure 23. Inclinometers.....	23
Figure 24. Data acquisition system .....	23
Figure 25. Deck deformation: load case 1.....	25
Figure 26. Deck deformation: load case 2.....	25
Figure 27. Deck deformation: load case 3.....	25
Figure 28. Deck deformation: load case 4.....	26
Figure 29. Deck deformation: load case 5.....	26
Figure 30. Deck deformation: load case 6.....	26
Figure 31. Measurement points .....	27
Figure 32. Equipment for vibration test .....	28
Figure 33. Acceleration acquisition program .....	28
Figure 34. Transverse acceleration at the mid spans.....	29
Figure 35. Vertical acceleration at the mid spans .....	29





Figure 36. 1 <sup>st</sup> Singular values spectra of the transverse records.....	30
Figure 37. 1 <sup>st</sup> Singular values spectra of the vertical records.....	30
Figure 38. Comparison of identified and calculated frequencies .....	31
Figure 39. 1 <sup>st</sup> transverse mode .....	33
Figure 40. 2 <sup>nd</sup> transverse mode .....	33
Figure 41. 3 <sup>rd</sup> transverse mode.....	34
Figure 42. 4 <sup>th</sup> transverse mode.....	34
Figure 43. 1 <sup>st</sup> vertical mode .....	34
Figure 44. 2 <sup>nd</sup> vertical mode .....	35
Figure 45. 3 <sup>rd</sup> vertical mode.....	35
Figure 46. 4 <sup>th</sup> vertical mode.....	35
Figure 47. 5 <sup>th</sup> vertical mode.....	36
Figure 48. 1 <sup>st</sup> torsional mode.....	36
Figure 49. 2 <sup>nd</sup> torsional mode .....	37
Figure 50. 3 <sup>rd</sup> torsional mode .....	37
<i>Figure 51. Prototype Configuration 1 overview.....</i>	<i>40</i>
<i>Figure 52. Prototype Configuration 2 overview.....</i>	<i>40</i>
<i>Figure 53. Prototype Configuration 3 overview.....</i>	<i>41</i>
Figure 54. Connection piece (original design from PS35) .....	43
Figure 55. General layout of the prototype .....	44
Figure 56. Prototype setup for in-lab tests .....	45
Figure 57. Rear restraining system for the prototype.....	45
Figure 58 – Cross-section view of the laboratory assembly.....	47
Figure 59. Instrumentation setup overview .....	48
Figure 60. Detail of the instrumentation in the connection zone.....	49
Figure 61. Location of the acquisition sensors in the cross-section.....	49
Figure 62. Concrete Box girder cross-section.....	53
Figure 63. External formwork.....	53
Figure 64. Formwork and reinforcement of the upper deck slab .....	53
Figure 65. Freshly concreted upper deck slab.....	54
Figure 66. Construction details for the prototype .....	54
Figure 67. Steel structure of the box section .....	55
Figure 68. Metallic structure of the box section .....	55
Figure 69. Suspension eyebolts with tie rods.....	56
Figure 70. Support beam for the prototype of the test .....	56
Figure 71. Rear restraining system for the prototype.....	57



Figure 72. Distribution beam for the hydraulic jack in the test .....	57
Figure 73 and Figure 74. Installing the eyebolts for prototype mobilization and weighing .....	58
Figure 75. Prototype transportation .....	58
Figure 76. Prestressing the prototype in the laboratory .....	59
Figure 77. Prototype stored in the POTD .....	59
Figure 78. Instrumentation assembly at LNEC's premises .....	60
Figure 79. Instrumentation, control systems setup and calibration .....	60
Figure 80. Instrumentation: strain gauges and clinometers .....	61
Figure 81. Laboratory – Prototype being tested – front view .....	61
Figure 82. Laboratory – another view of the prototype during the tests .....	62
Figure 83. Laboratory – Prototype being tested – back view .....	62
Figure 84. Load-displacement curve for the Configuration 1 .....	63
Figure 85. Load-displacement curves for Configurations 2 & 3 .....	64



# 1 Introduction

The digital upgrade of construction works presents itself as mandatory in the forthcoming years. While its need is transversally recognized by the construction industry, the same will face meaningful challenges in terms of competitiveness among its players, as well as regarding other sectors of the economy, until this upgrade proves itself as effective. Similarly, all efforts that may lead to either standard, modular or out-of-site prefabrication solutions will strengthen the outcome of digital integration, once it points out to lean, previewed and monitored interventions performed on the construction sites.

Despite the wide road network already built in the modern world, in Europe moreover, the need for new bridges is a permanent pursuit. New road crossings, either for roadways, for new pedestrian and bicycle routes or for fauna crossings, are a constant need. Also, widening existing roads to accommodate higher traffic demands, results in the need for new under- and overpasses.

Hybrid bridges are a concept wherein bridges are designed with a combination of different materials but at different locations in the structure, unlike the usual composite behaviour where the materials are combined at a cross-section level. The different parts of the structure share a continuous joint, responsible for the transmission of mechanical forces.

In this type of bridge, accurate planning and design processes, considering all the existing constraints and construction phases, are the key factors to allow a functional use of robotised equipment and to perform automated construction.

Meanwhile, the usability lifecycle of many road infrastructures is also a challenge that needs to be faced in the forthcoming years and bridges are usually infrastructures whose requirements of maintenance and retrofitting generally have a strong impact on the infrastructure's lifecycle.



## 2 Objectives

The objective of task T4.1 is the development of enhanced modular solutions for pre-manufactured bridges for overpasses that minimizes the construction site operations, especially the works that take place above the traffic lanes, which are kept under circulation.

Particularly, the scope of this task is the design of a modular and hybrid solution for bridges, focusing mainly on highway overpasses, through optimization of the assets and methods used in bridge construction and an increased industrialization level by introducing optimized processes in the bridge components production pipeline.

During the development of this task, one of the main goals is to revise and enhance the design of the connection elements between the steel and concrete parts in order to ensure its robustness performance-wise and safety-wise. This will allow to minimize the adjustments required to make a more general use of this solution such as in scenarios with different span arrangements.

A campaign comprising load tests on an existing structure, lab tests on prototype models, and structural analyses with analytical models were carried out in order to develop this improved design.

Another goal of this task is to improve the production processes of the steel parts, by providing alternative designs that may speed-up the manufacture and take advantage of already existing automated, mechanized workshop methods.



*Figure 1. Steel Structure*

### 3 Background. Modular solution for pre-manufactured bridges

One of the most commonly used solutions in highway infrastructures is the prestressed concrete girder. It presents itself as an economic and adaptable solution, used throughout a variety of different settings.

Some disadvantages are the fact that their construction required the erection of support structures in the vicinity of the road, traffic must be interrupted for several hours during concreting operations and usually there were severe constraints in terms of width of the roadway and/or number of operational lanes in the highway for an extended period of time.

Over the years there was a shift towards the enforcement of an increased safety level during construction and maintenance of highway infrastructures which required measures to reduce the risk of accidents, by limiting the number of workers on site, avoiding certain riskier types of works and, also, reducing the interference with the normal flow of traffic.

Among the possible solutions that were sought to meet some of these requirements, the following can be highlighted:

**Steel-Concrete girders.** The use of steel beams with concrete slabs allows for a very simple and fast construction, while minimizing the interference with traffic and the amount of manual labour on site. But they also present a disadvantage: the trade-off of replacing concrete by steel has a price: overall increased costs and high-maintenance requirements.



*Figure 2. Steel-Concrete girders. Bottom view.*



Figure 3. Steel-Concrete girders. Side view.

**Precast Concrete girders:** While being very similar to the previous steel-concrete solution in terms of safety, simplicity and speed of construction while keeping interference with the main highway to the minimum, structurally speaking, these solutions, for the same bridge spans, require much higher beams, therefore requiring a specific road design to prevent clearance issues. Also, structures using these solutions often have a more pronounced and heavier visual appearance than the other solutions.



Figure 4. Examples of Precast Concrete girders

**Hybrid bridge:** This solution lies in the middle ground and is the one being proposed in this task. A structure that is simple, fast and safe to build and aims to be more efficient from both a structural and constructive points of view. This stems from the fact that both concrete and steel are employed in different areas of the bridge in a way that maximizes their structural effectiveness.

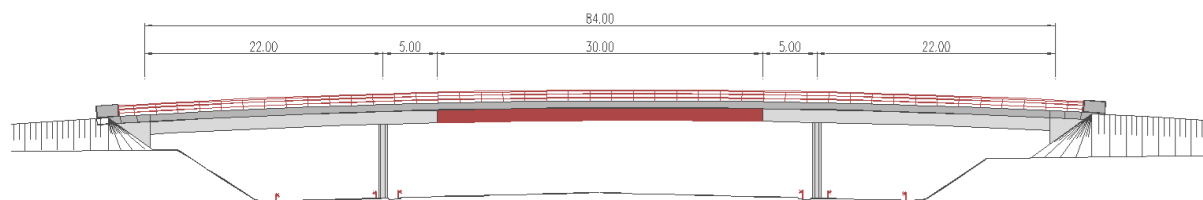


Figure 5. Hybrid Bridge



Figure 6. A Hybrid Bridge. Side and Bottom views.

This procedure could be used for a new construction or during the process of widening the main highway (as shown in the example) or the overpasses themselves.



Figure 7. Widening the main highway (A3, Portugal)

Construction-wise, it leverages the use of premanufactured components to a greater extent (precast concrete girders and pre-assembled steel span) and, as in the previous solutions, it takes advantage of the prefabrication, reduced number of workers on site and a minor risk of accidents due to very short periods of traffic interruptions.

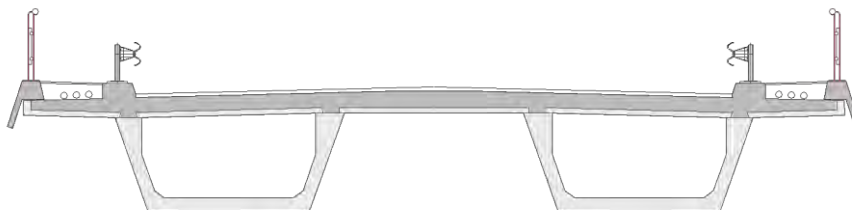


Figure 8. Precast concrete girders and pre-assembled steel span

The following images illustrate an example procedure for the replacement of a set of overpasses during the process of widening the main highway profile.



Figure 9. Construction procedure – 1 (Precast segments and steel structure assembly)



Figure 10. Construction procedure – 2 (Concrete slab and final demolition of existing structure)

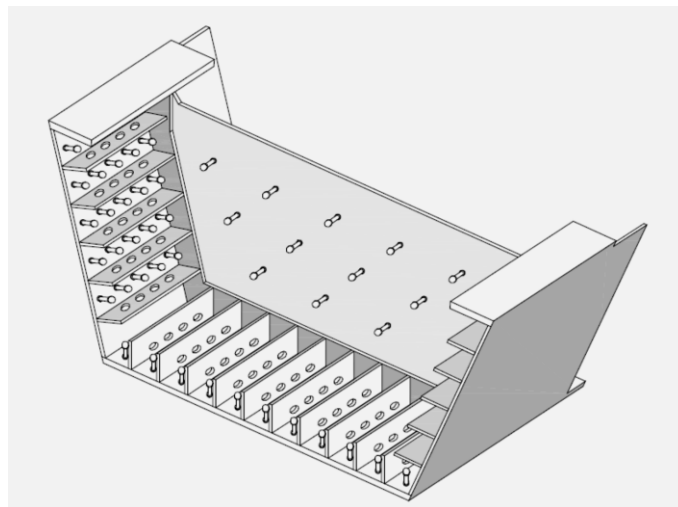


Figure 11. Connection element between the steel and concrete parts (Armando Rito, 2012)

In the context of the OMICRON project, this solution, which has already been successfully used in some stretches of highways in Portugal, is to be incorporated in the methodology due to its capability to meet the requirements of safety for the construction and maintenance of road infrastructures, and as mentioned before, because of all its constructive advantages.



## 4 Static and Dynamic Load Tests

In the context of the OMICRON project, the role played by the hybrid solutions is to represent the construction part of the lifecycle of the roadways and one of the tasks is to further develop the solution to enhance the construction process, with increased safety and efficiency and focusing particularly on the connection.

The interface between the concrete beams and their steel counterparts is one of the critical aspects of this solution since the connection must transfer adequately the stresses from one material to the other and maintain structural continuity along the span.

Before further developments, and taking advantage of the fact that there are overpasses with this structural solution already in existence, a set of static load and ambient vibration tests were carried out to evaluate the structural behaviour of the solution used in this connection. For this purpose, the overpass PS35 at the A3 Highway - Porto/Valença was selected as case study.

### 4.1 Description of the overpass PS35

The PS35 overpass is located in the Maia/Santo Tirso sub-ramp of the A3 Highway at km 16+860 and connects Bouça da Francisca and Querelelo locations.

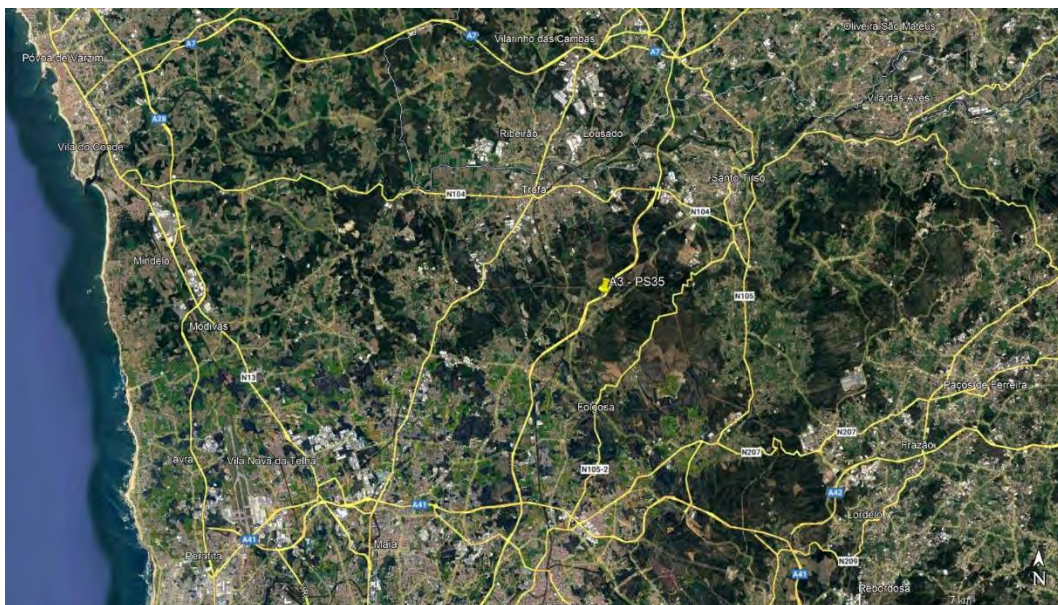


Figure 12. PS35 location

As part of the widening to 2x4 lanes of the Maia / Santo Tirso branch of the A3 Highway, it became necessary to replace all the existing overpasses since they were not corresponding to the new highway section.

The hybrid steel-concrete deck solutions were applied to minimize the in-situ construction operations and maintain traffic circulation on the highway. Due to the ratio between side spans and main span, the adopted structural solution for overpasses comprised two central span longitudinal steel box-girders. These girders are connected to and continuous with two concrete precast beams in the remaining main span length and in the side spans, providing an excellent aesthetic appearance.



Located at km 16+871,841 of the A3 Highway - Porto/Valença, Maia/Santo Tirso branch, with a total length of 76 m, the overpass PS35 consists of 3 spans, with two 18 m side spans and a 40 m central span (Figure 5). The overpass crosses the entire highway with a 6.3 m gauge (Figure 14) and the deck is 9.70 m wide, supporting two traffic lanes.



*Figure 13. Elevation view of the overpass PS35*

The side spans use precast prestressed concrete elements whereas the central span is a steel-concrete composite structure (Cabral, Bispo, & Rito, 2012). Thus, the deck is made up of a pair of prefabricated “U” beams in pre-tensioned concrete on top of which pre-slabs are placed prior to casting the concrete for the top slab (Figure 15). These beams extend 5 m in cantilever into the central span on each side of the piers where the steel “U” beams will connect. The exterior geometry of the steel beams is identical to that of the prefabricated concrete beams. Similarly, to the precast side spans, the construction of the central span is completed by the placement of pre-slabs and concreting of the top slab.

The connection between the central metallic section and the concrete section is made using a metallic piece that is integrated in the concrete through connectors embedded in a septum at the end of the concrete beam, as shown in Figure 16. The bridge is supported monolithically by two pairs of piers in reinforced concrete, with a constant cross-section along the height. The cross-section has an “I” shape with external dimensions of 0.80 x 2.00 m.



*Figure 14. Bottom view of the overpass*





Figure 15. Overpass Cross-sections (Armando Rito, 2012)

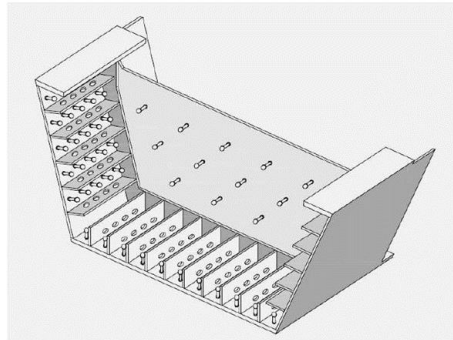


Figure 16. Connection between the steel girders and the precast beams (Armando Rito, 2012)

## 4.2 Numerical model

A finite element model for the overpass PS35 was developed to evaluate its response to the static and dynamic tests. The FE model was built using the software RM v8i (Bentley).

The FE model is totally based on 3D frame elements. Two parallel main beam alignments represent both concrete and steel beams, connected by transversal elements that simulate the behaviour of the top slab in a simplified manner. As a simplification, the internal bracing system within the steel parts was not modelled, although its mass was considered in the dynamic analysis.

A general perspective of this model is presented in Figure 17.

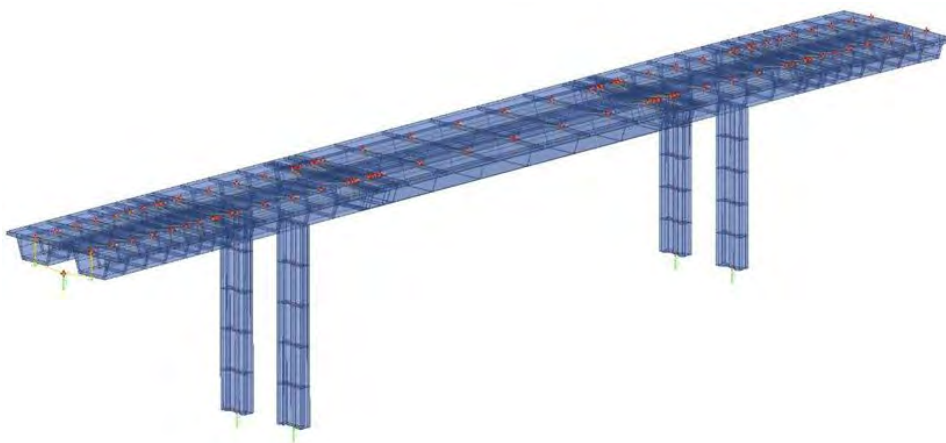


Figure 17. Perspective of Finite element model (3D Beam)

Prior to the actual on-site load tests, the FE model was used to estimate the deformation of the structure on static loads and the natural vibration mode shapes.

After the tests, the FE model was calibrated with the static load tests results, at first, and then adjusted to the dynamic characteristics identified from the dynamic tests.

The concrete used in the construction of precast beams, cast in situ piers, abutments and concrete slabs had different specifications due to their distinct requirements and thus, their modulus of elasticity also varies, ranging between 42.9 and 48 GPa. The total mass of the structural elements is 1860 tons, and the additional mass is 350 kg/m, corresponding to the mass of the lateral sidewalks and the guard rail. The stiffness of the link elements to model the supports at the abutments was adjusted to fit the computed modal characteristics to the ones identified from the tests.

## 4.3 Static Load Tests

### 4.3.1 Testing procedure

The static load tests were carried out using 4 loaded trucks (Figure 18). The truck’s characteristics are summarized in Table 1. The total weight of the trucks was 997 kN.

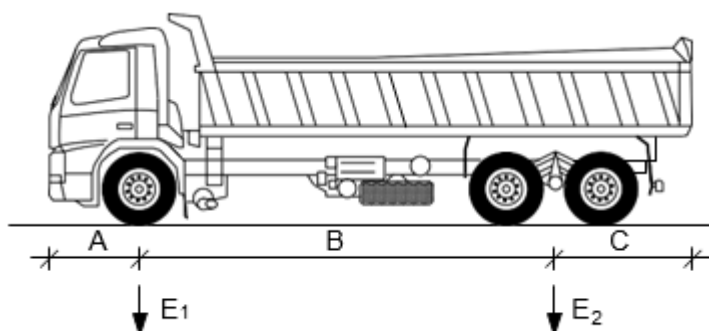


Figure 18. Geometric definition of the trucks

Table 1. Weights and lengths of the trucks

Truck	Register	Weight (kN)			Length (m)		
		Total	E1	E2	A	B	C
1	24RM75	248.2	87.3	160.9	1.6	4.5	2.1
2	1390MZ	244.6	71.5	173.1	1.3	4.4	1.6
3	6314MV	249.7	68.1	182.1	1.6	3.7	1.9
4	66LF72	254.0	73.3	180.7	1.4	4.5	2.1

These trucks were placed in six positions (Figure 19) aiming to evaluate the behaviour of the connections.

In the first three cases, 2 trucks were lined up and placed successively at the mid-span sections to obtain significant vertical displacements (Figure 20).

In the 4<sup>th</sup> and 5<sup>th</sup> loading cases, 4 trucks were used, which were placed on two adjacent mid-spans simultaneously to induce important bending moments in the support sections (Figure 21).

Finally, in the last load case, the trucks were placed back-to-back, at the location above both steel-concrete connections.

	E1	P1	P2	E2
1	1 2			
2		1 2		
3				1 2
4	3 4	1 2		
5		3 4		1 2
6		3 4	1 2	

Figure 19. Load cases considered in the tests



Figure 20. Trucks at the mid span (Load case 1)



Figure 21. Trucks at the adjacent mid span (Load case 4)

### 4.3.2 Equipment

During the load tests, the structural behaviour was monitored by measuring vertical displacements and rotations.

The measurement of vertical displacements was carried out using 6 units of UniMeasure JX-P420 series linear position measuring transducer (UniMeasure, 2011). The transducer is a loop powered device with a 4 to 20 mA current output with a measurement range of 500 mm. A resolution is 0.0004 mA, limited by DataTaker series DT80 (Thermo Fisher, 2013), what is corresponding to 0.01 mm.

These transducers are placed in the three mid-span sections of the overpass, two for each section (Figure 22). To assess the connections between the steel girders and the concrete beams, the rotations of the steel beams and the concrete beam at locations close to the joints were monitored (Figure 23). The transversal and longitudinal rotations were measured by two-axis gravity referenced inclinometers Schaevitz T233/T235 with a measurement range of  $\pm 3$  degree (Sherborne Sensors, 2002). The resolution is of about 0.2 arcseconds. In total, 8 inclinometers were installed.

The air temperature was also measured using a thermometer type Pt100.

The data acquisition of all the sensors installed was performed by a datalogger Datalogger DT80G with an expansion module CEM 20 (Thermo Fisher, 2013) (Figure 24).

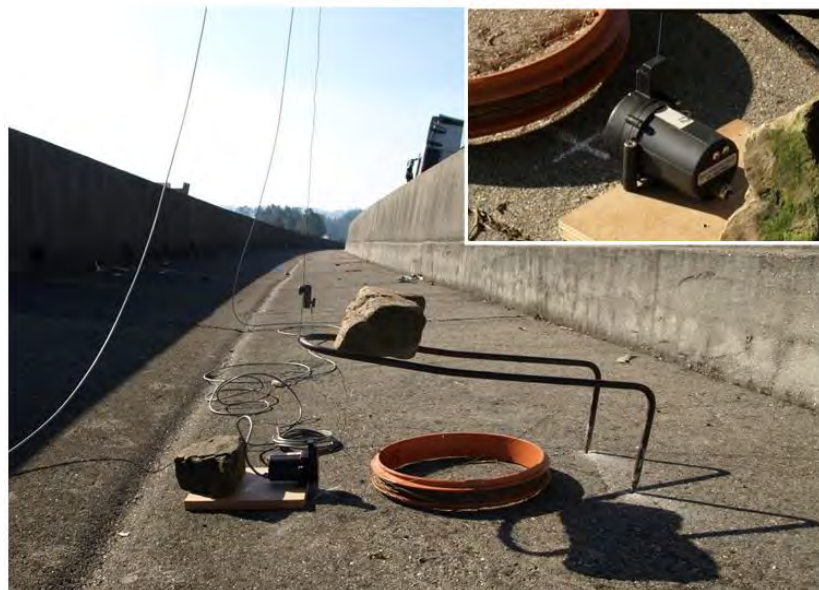


Figure 22. Linear position measuring transducer

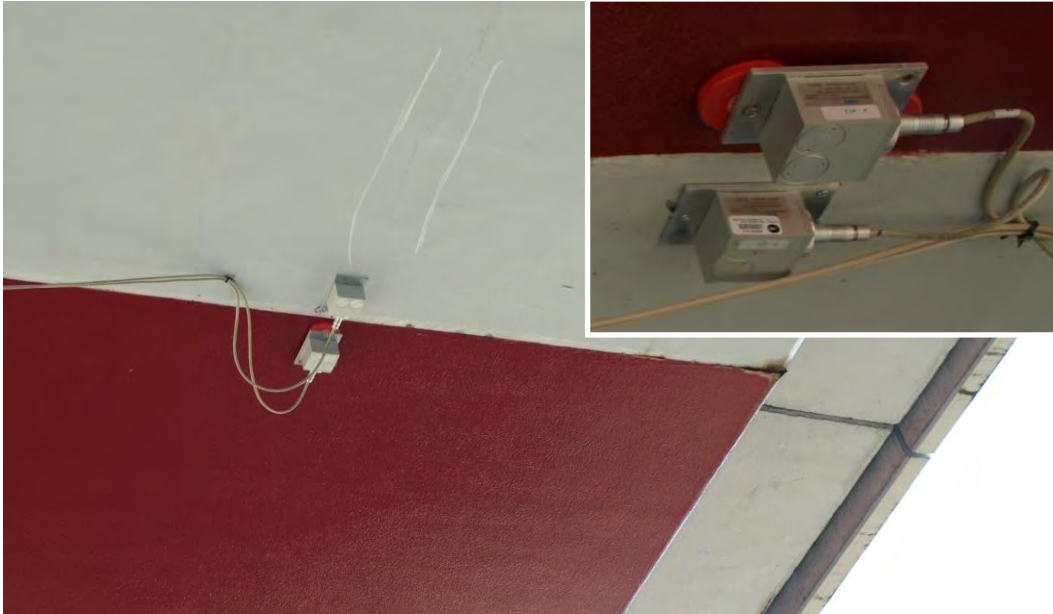


Figure 23. Inclinometers



Figure 24. Data acquisition system

During the tests, the sample rate was 0.2 Hz. For each load position, a minimum of 8 stabilized measurements were recorded. Before and after the load tests and between the 3<sup>rd</sup> and 4<sup>th</sup> load cases, the measurements for structural state “Zero” (without any load) were taken.

### 4.3.3 Main results

The load tests took place between 9:00 and 10:30 am on November 12<sup>th</sup>, with an ambient temperature that varied between 9.5°C and 12.0°C.



The vertical displacements and the rotations measured during the static load tests are presented in Table 2 and Table 3. For comparison the tables also include the results interpreted from the three-dimensional finite element model.

Table 2. Vertical displacements (mm)

Load case		D1	D2	D3	D4	D5	D6
1	Measured	0.7	0.7	0.1	-0.2	0.0	-0.1
	Calculated	0.7	0.7	-0.5	-0.5	0.0	0.0
2	Measured	-0.3	-0.3	4.8	5.1	-0.2	-0.4
	Calculated	-0.5	-0.5	5.7	5.7	-0.5	-0.5
3	Measured	0.0	0.0	0.0	-0.2	0.2	0.3
	Calculated	0.0	0.0	-0.4	-0.4	0.7	0.7
4	Measured	0.2	0.2	4.5	4.8	-0.3	-0.5
	Calculated	0.2	0.2	5.2	5.2	-0.5	-0.5
5	Measured	-0.3	-0.3	4.9	5.1	0.1	0.0
	Calculated	-0.5	-0.5	5.2	5.2	0.1	0.1
6	Measured	-0.4	-0.4	4.2	4.5	-0.3	-0.6
	Calculated	-0.7	-0.7	5.4	5.4	-0.7	-0.7

Table 3. Longitudinal rotations (arc seconds)

Load case		Connection 1				Connection 2			
		CL.1	CL.3	CL.2	CL.4	CL.5	CL.7	CL.6	CL.8
1	Measured	-12	-12	-13	-12	5	5	7	3
	Calculated	-12		-12		4		4	
2	Measured	50	49	50	50	-52	-52	-52	-61
	Calculated	56		56		-63		-63	
3	Measured	-4	-4	-4	-5	11	10	10	10
	Calculated	-4		-4		10		10	
4	Measured	37	38	39	39	-49	-50	-50	-51
	Calculated	44		44		-58		-58	
5	Measured	51	52	51	52	-47	-48	-45	-46
	Calculated	53		53		-53		-53	
6	Measured	65	63	64	62	-60	-63	-60	-64
	Calculated	72		72		-73		-73	





The significant displacements were, naturally, observed at the mid-span of the central span, as shown from Figure 25 to Figure 30. The maximum value was 5.1 mm, measured during load case 5.

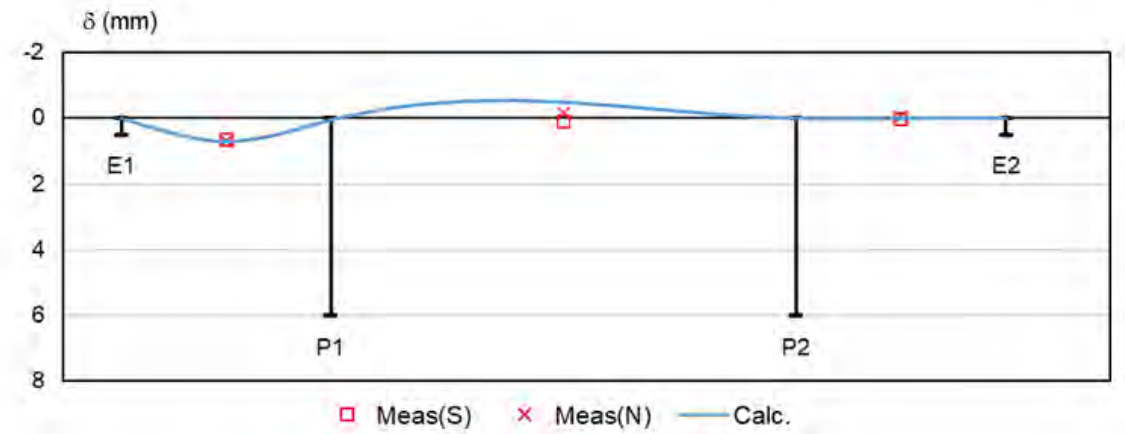


Figure 25. Deck deformation: load case 1

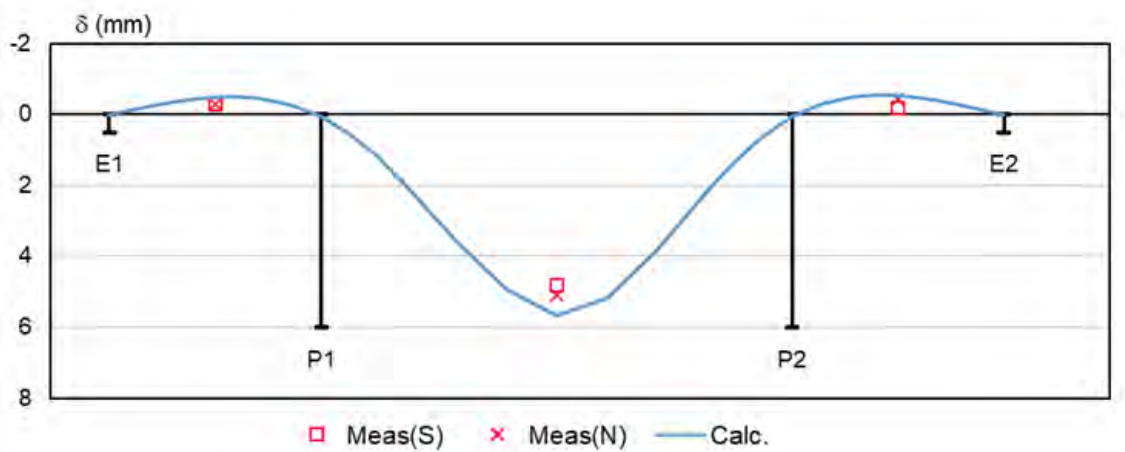


Figure 26. Deck deformation: load case 2

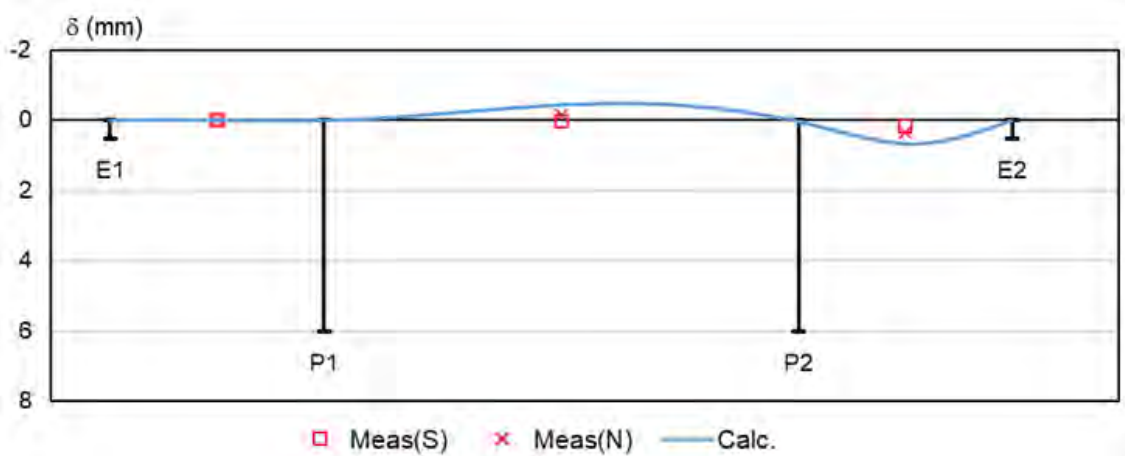


Figure 27. Deck deformation: load case 3

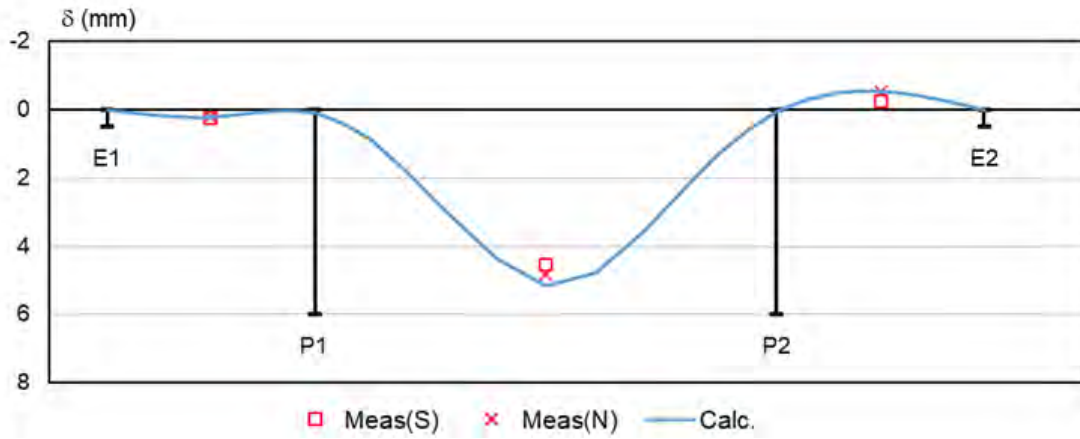


Figure 28. Deck deformation: load case 4

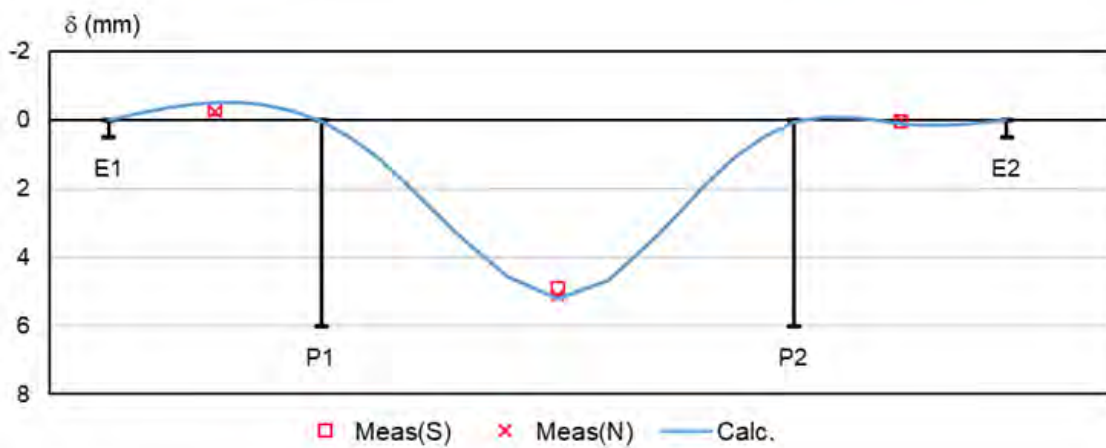


Figure 29. Deck deformation: load case 5

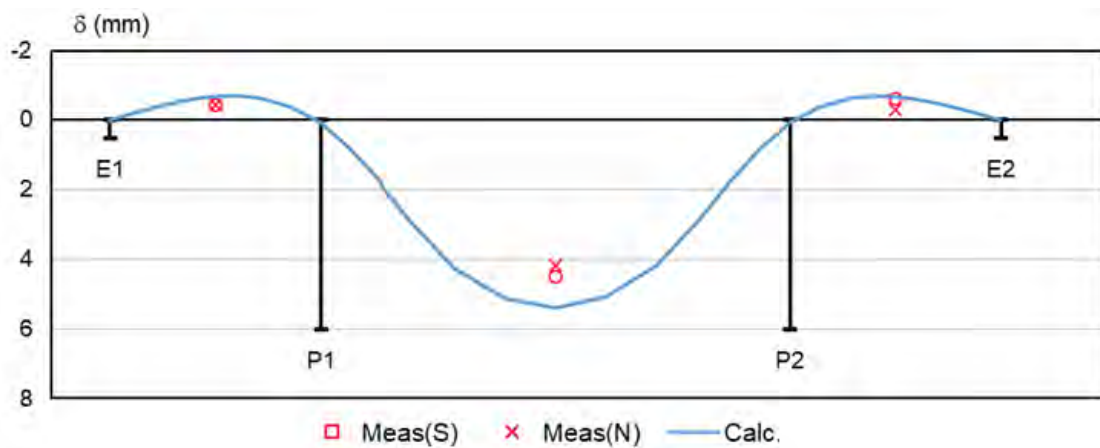


Figure 30. Deck deformation: load case 6

The longitudinal rotations measured simultaneously in the concrete and metallic beams, near the connections, were basically the same, meaning the connections behaved monolithically. The maximum rotations, about 60" to 64", took place for the 6<sup>th</sup> load case, in which the trucks were placed above the connection sections.

## 4.4 Dynamic tests

### 4.4.1 Testing procedure

Dynamic tests are performed to evaluate the dynamic characteristics of the structure, namely its frequencies, mode shapes and damping coefficients. Therefore, the ambient vibration test of the overpass was carried out, without a traffic interruption. The structural vibration was caused, essentially, by wind and highway traffic below the overpass. For the analysis, the main modal parameters provided by the ambient vibration test were compared with the corresponding parameters predicted by the numerical model.

The tests were carried out in 3 setups with 12 uniaxial accelerometers (Table 4), placed successively along the deck (Figure 31). In the first setup the transverse accelerations were measured. In the other two setups the vertical and longitudinal accelerations were acquired. In each setup the accelerations were measured for a duration of 40 minutes, with a sampling rate of 500 Hz. The tests took place between 10 am and 3 pm on November 11th, with an average ambient temperature 19°C.

Table 4. Dynamic test setups (T-transverse direction; V-vertical direction)

Setup	Group 1			Group 2			Group 3			Group 4		
	Cn1	Cn2	Cn3	Cn1	Cn2	Cn3	Cn1	Cn2	Cn3	Cn1	Cn2	Cn3
1	1T	3T	–	6T	7T	8T	9T	10T	11T	12T	13T	15T
2	2V	3V	4V	5L	7V	8V	9V	10V	11L	12V	13V	14V
3	16V	17V	18V	6V			19V	20V	21V	22V	23V	24V

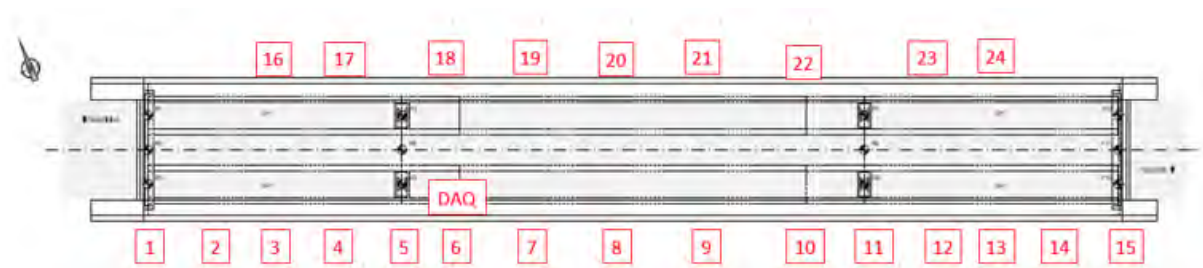


Figure 31. Measurement points

### 4.4.2 Equipment

The ambient vibration tests were carried out using the following equipment (Figure 32):

- 12 Kinematics Uniaxial Episensor (ES-U) accelerometers (Kinematics, 2000).



- Four power supplies and signal conditioning units, developed by LNEC.
- Data acquisition equipment from Gantner Instruments (Gantner, 2009).

The ES-U accelerometers were force balance acceleration sensors from Kinometrics. They have a high dynamic range (greater than 145 dB) and low noise performance. Their bandwidth ranges from DC to 200 Hz. In the ambient vibration tests performed on the Overpass PS35, the ES-U accelerometers were configured with a sensitivity of 20 Volt/g and the gain factor at the power supply and signal conditioning units was configured to 5. With this configuration, the minimum acceleration amplitude that could be measured was 0.381  $\mu\text{g}$ .

The data acquisition was performed with a program developed in LabView (NI, 2008) (Figure 33)

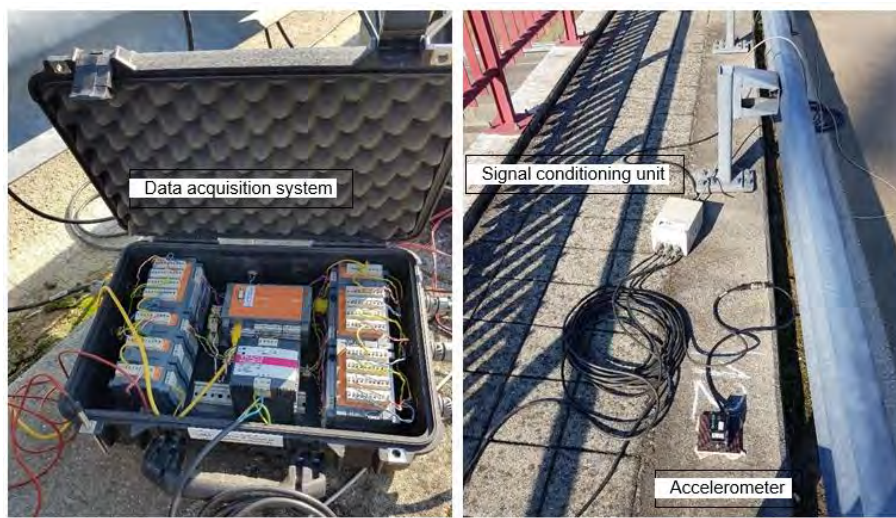


Figure 32. Equipment for vibration test

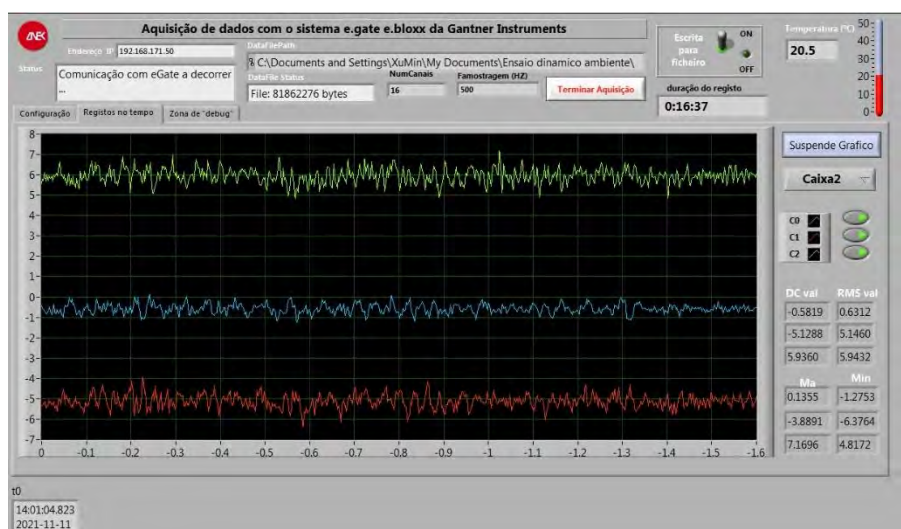


Figure 33. Acceleration acquisition program

### 4.4.3 Modal identification

Before the modal identification process, the records acquired with a sampling frequency of 500 Hz were pre-processed with low-pass filtering at 20 Hz using an 8 poles Butterworth filter and decimation to a sampling frequency of 50 Hz.

For instance, Figure 34 and Figure 35 present the pre-processed transverse and vertical accelerations acquired at the first and second mid-spans. As shown, the transverse vibration levels are similar in all spans, however, the vertical vibration level in the central span is much higher than in the lateral spans.

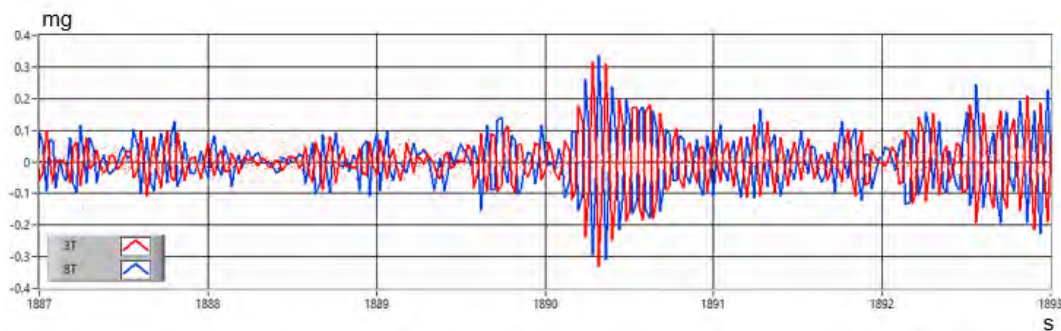


Figure 34. Transverse acceleration at the mid spans

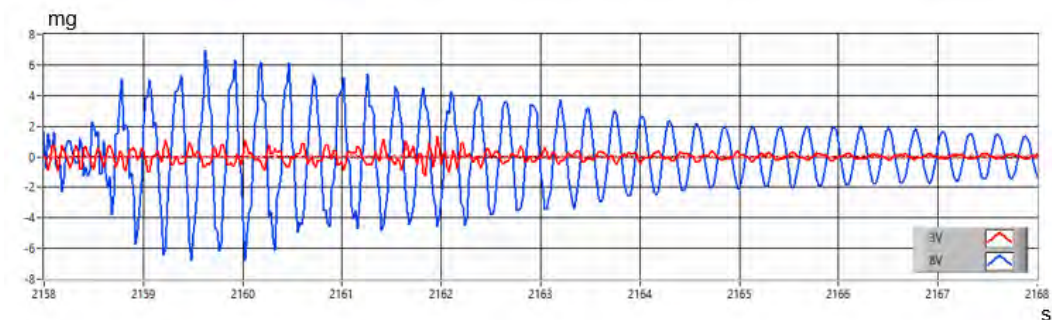


Figure 35. Vertical acceleration at the mid spans

The modal identification analysis of the Overpass PS35 was performed using a frequency domain output – only modal identification method – the enhanced frequency domain decomposition method (EFDD), implemented in the software ARTeMIS Extractor (SVS, 2005).

In the EFDD method, the spectral density functions matrix is, at each discrete frequency, decomposed in singular values and vectors (SVD). From the analysis of the singular values spectra, it is possible to identify the auto power spectral density functions corresponding to each mode of a system, which may include parts of several singular values spectra depending on which mode is dominant at each frequency. Generally, the dominant mode shows up at the 1st singular value spectrum and the other modes at the other singular values spectra. Additionally, the EFDD uses procedures to evaluate the damping and to get enhanced estimates of the frequencies and mode shapes of a system.

To apply the EFDD method to the data obtained in the ambient vibration tests of the Overpass PS35, the spectral density functions of the acceleration responses were estimated with the Fast Fourier transform (FFT) algorithm applied to windowed and overlapped samples with 1024 values each. Since the sampling frequency of the records is 50 Hz (after pre-processing) the frequency resolution of the estimated spectra is 0.024 Hz.



Figure 36 shows the spectra of the first singular values of the spectral density functions matrices of the measured transverse accelerations. The frequencies corresponding to the most evident resonance peaks in the 1<sup>st</sup> singular value spectrum are also shown in Figure 36. On these resonance peaks, the 4 transverse vibration modes were identified. In the same way, Figure 37 shows the averaged spectra of the first singular values of the spectral density functions matrices of the measured vertical and longitudinal accelerations and the frequencies of the 8 identified vertical and torsional modes.

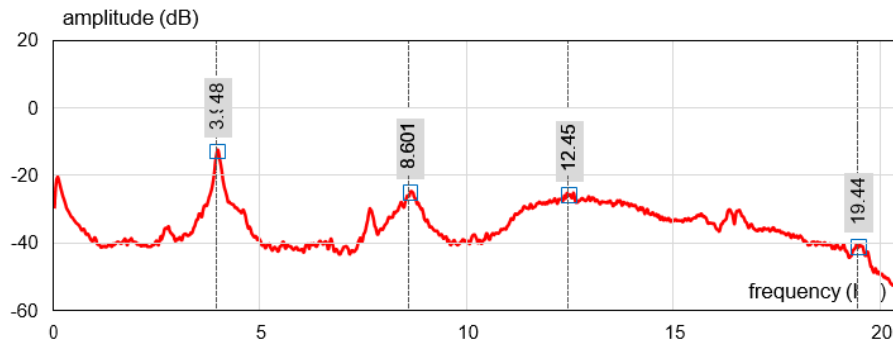


Figure 36. 1<sup>st</sup> Singular values spectra of the transverse records

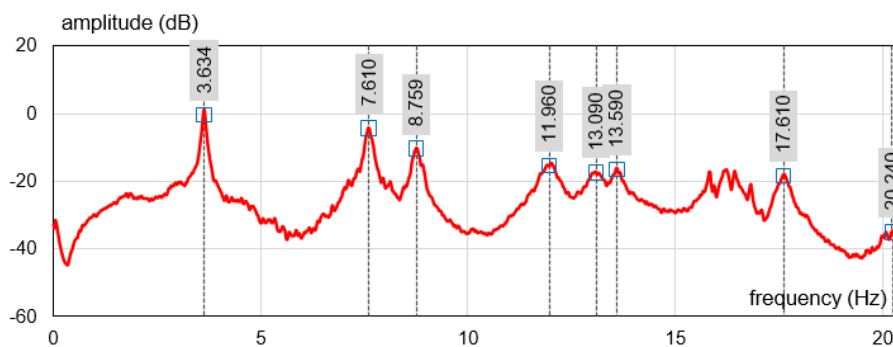


Figure 37. 1<sup>st</sup> Singular values spectra of the vertical records

Table 5 shows the frequencies and damping ratios of the natural modes identified from the vibration tests, as well as the corresponding frequencies calculated by the numerical model. The table also includes the Modal Assurance Criterion (MAC), which estimates a similarity between the mode shapes obtained from the test and the calculated. The Values MAC mostly are greater than 0.8, which means a good similarity is achieved.

For visual comparison, Figure 38 presents the identified and calculated frequencies in graphic. If the identified frequencies are equal to the calculated, the points should be on the diagonal line. As shown, the numeric model can simulate very well the transverse and torsional modes, even though for the vertical modes the model is more flexible than the real structure.

Table 5. Identified vibration modes

Mode	Experimental		Calculated	MAC
	f (Hz)	$\epsilon$ (%)	f (Hz)	
<b>Transverse Modes</b>				



Mode	Experimental		Calculated f (Hz)	MAC
	f (Hz)	$\epsilon$ (%)		
1	3.948	1.16	3.464	0.977
2	8.601	2.75	7.696	0.830
3	12.450	4.53	12.772	0.692
4	19.440	0.47	20.625	0.642
<b>Vertical Modes</b>				
1	3.634	0.81	2.885	0.996
2	8.759	1.04	6.497	0.903
3	11.960	1.45	8.705	0.933
4	13.090	0.90	8.888	0.963
5	17.610	0.72	12.772	0.524
<b>Torsion Modes</b>				
1	7.610	0.81	7.453	0.968
2	13.590	0.68	13.519	0.688
3	20.240	0.79	18.598	0.436

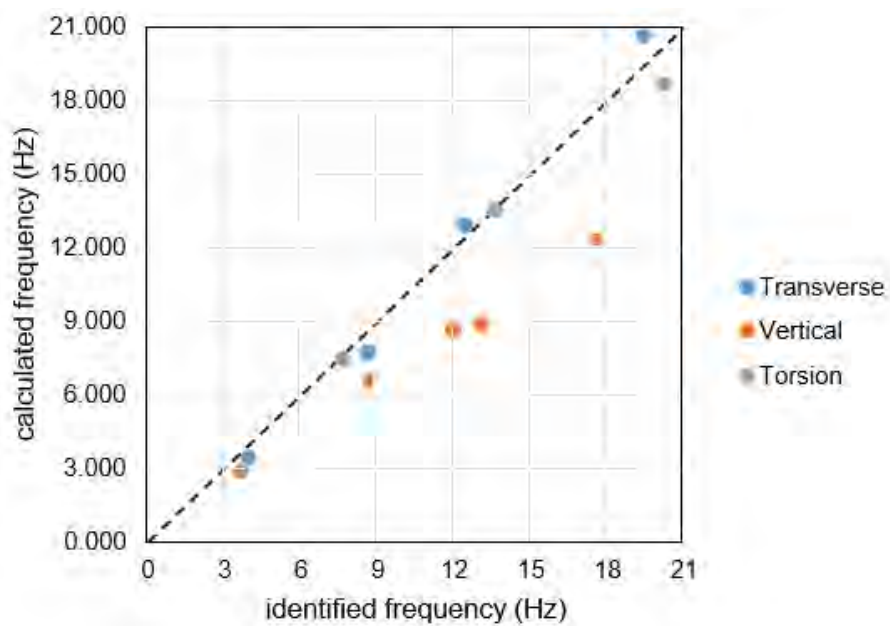


Figure 38. Comparison of identified and calculated frequencies

Table 6 presents the modal components of the transverse vibration modes and Table 7 presents the vertical and torsional modes' components. Figure 39 to Figure 50 show the modal configurations of the identified modes and the corresponding shapes output from the FEM model.



Table 6. Modal components of the transverse vibration modes

Mode	T1	T2	T3	T4
f (Hz)	3.948	8.601	12.45	19.44
$\varepsilon$ (%)	1.2	2.8	4.5	0.5
1T	0.095	-0.508	0.784	<b>1.000</b>
3T	0.361	-0.758	0.674	0.497
6T	0.806	-0.828	0.130	-0.519
7T	0.947	-0.531	-0.279	-0.512
8T	<b>1.000</b>	-0.027	-0.566	0.636
9T	0.939	0.510	-0.568	0.723
10T	0.796	0.860	-0.303	0.563
11T	0.671	0.987	-0.015	0.424
12T	0.522	<b>1.000</b>	0.302	-0.450
13T	0.399	0.992	0.562	-0.640
15T	0.104	0.727	<b>1.000</b>	-0.972

Table 7. Modal components of the vertical and torsional vibration modes

Mode	V1	V2	V3	V4	V5	TOR1	TOR2	TOR3
f (Hz)	3.634	8.759	11.956	13.086	17.610	7.610	13.593	20.242
$\varepsilon$ (%)	0.8	1.0	1.5	0.9	0.7	0.8	0.7	0.8
2V	-0.050	0.202	0.704	-0.443	-0.157	0.049	-0.110	0.117
3V	-0.068	0.280	0.840	-0.525	-0.158	0.066	-0.122	0.093
4V	-0.067	0.274	0.722	-0.447	-0.126	0.066	-0.088	-0.028
5L	-0.016	0.217	0.071	-0.085	0.057	0.015	-0.030	0.062
6V	0.236	-0.526	-0.167	-0.201	-0.625	-0.220	0.489	-0.632
7V	0.734	-0.991	0.120	-0.533	-0.203	-0.711	1.000	-0.229
8V	0.997	-0.050	0.517	0.030	1.000	-0.989	0.085	1.000
9V	0.765	1.000	0.045	0.544	-0.150	-0.752	-0.995	-0.226
10V	0.288	0.634	-0.266	0.216	-0.672	-0.283	-0.585	-0.760
11L	0.027	0.230	-0.017	-0.079	-0.066	-0.027	-0.046	-0.085
12V	-0.059	-0.253	0.573	0.523	-0.122	0.058	0.113	-0.029
13V	-0.078	-0.341	0.874	0.798	-0.194	0.076	0.181	0.117
14V	-0.051	-0.228	0.696	0.642	-0.181	0.050	0.149	0.151
16V	-0.112	0.324	1.000	-0.846	-0.193	-0.035	0.149	-0.046





Mode	V1	V2	V3	V4	V5	TOR1	TOR2	TOR3
17V	-0.082	0.223	0.601	-0.500	-0.111	-0.019	0.076	0.020
18V	0.249	-0.530	-0.153	-0.219	-0.620	0.262	-0.507	0.476
19V	0.733	-0.946	0.138	-0.552	-0.212	0.749	-0.932	0.227
20V	1.000	-0.069	0.518	-0.054	0.935	1.000	-0.108	-0.810
21V	0.762	0.988	0.007	0.566	-0.170	0.747	0.926	0.180
22V	0.283	0.617	-0.260	0.219	-0.628	0.278	0.547	0.612
23V	-0.087	-0.234	0.505	0.596	-0.143	-0.002	-0.135	0.058
24V	-0.115	-0.339	0.842	1.000	-0.233	-0.009	-0.243	0.025

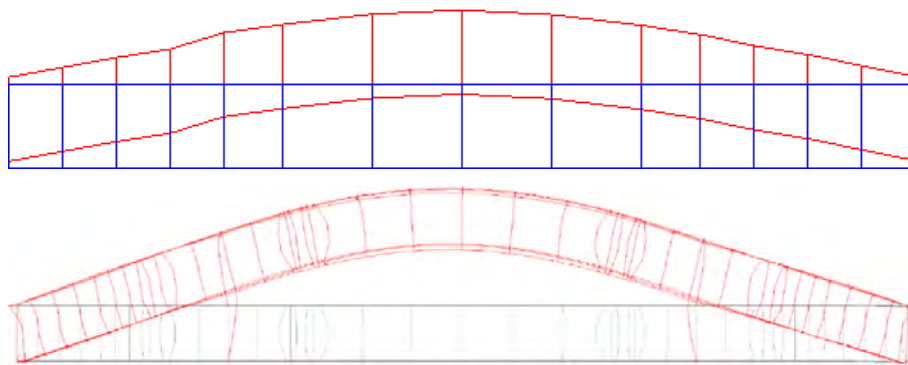


Figure 39. 1<sup>st</sup> transverse mode

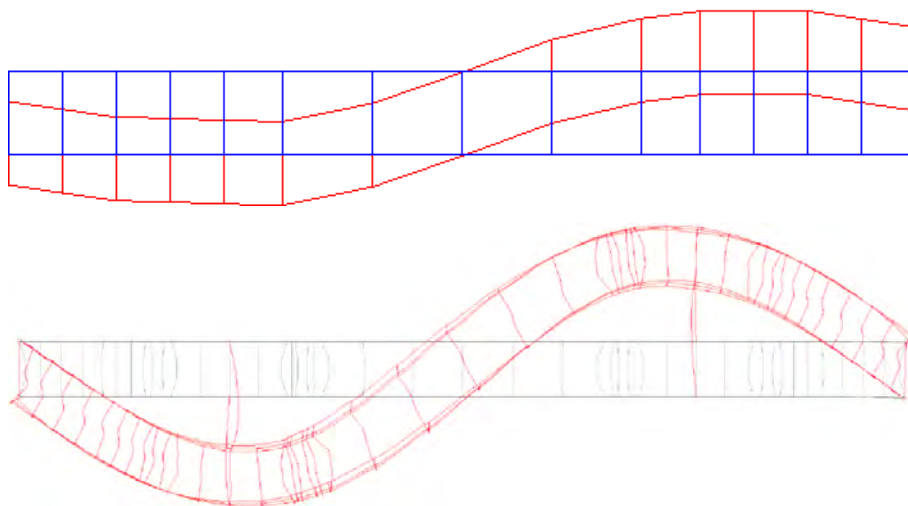


Figure 40. 2<sup>nd</sup> transverse mode

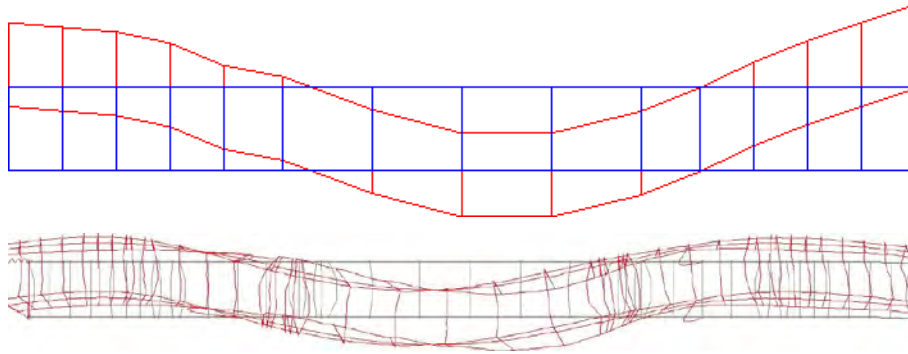


Figure 41. 3<sup>rd</sup> transverse mode

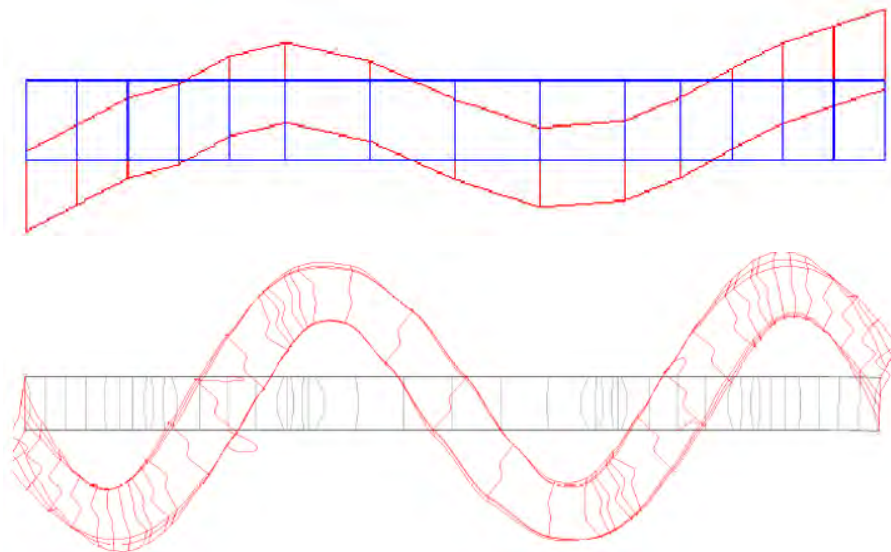


Figure 42. 4<sup>th</sup> transverse mode

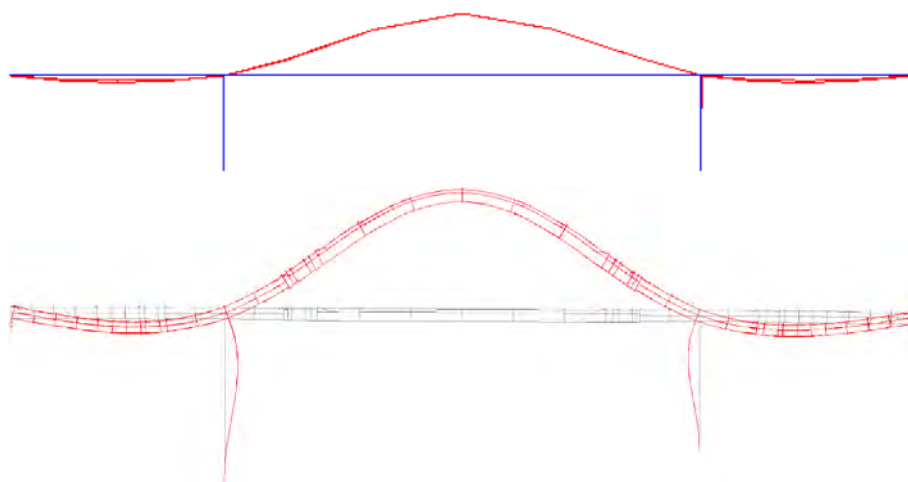


Figure 43. 1<sup>st</sup> vertical mode

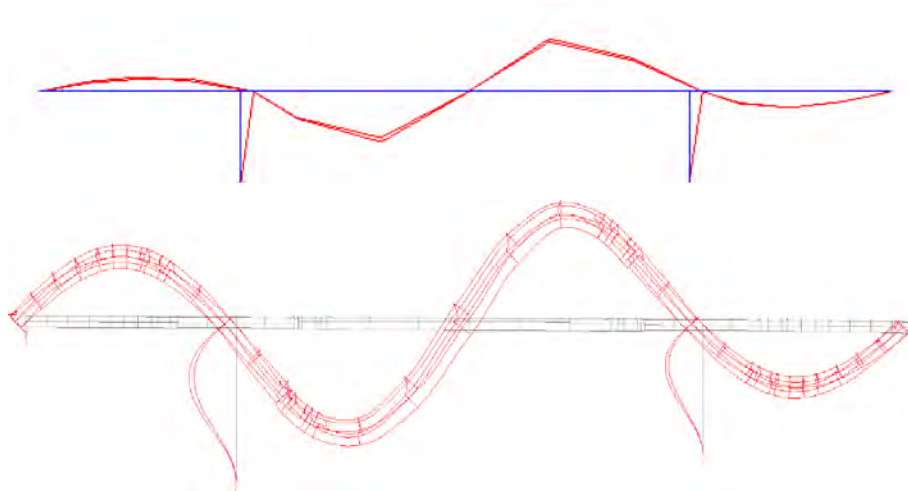


Figure 44. 2<sup>nd</sup> vertical mode

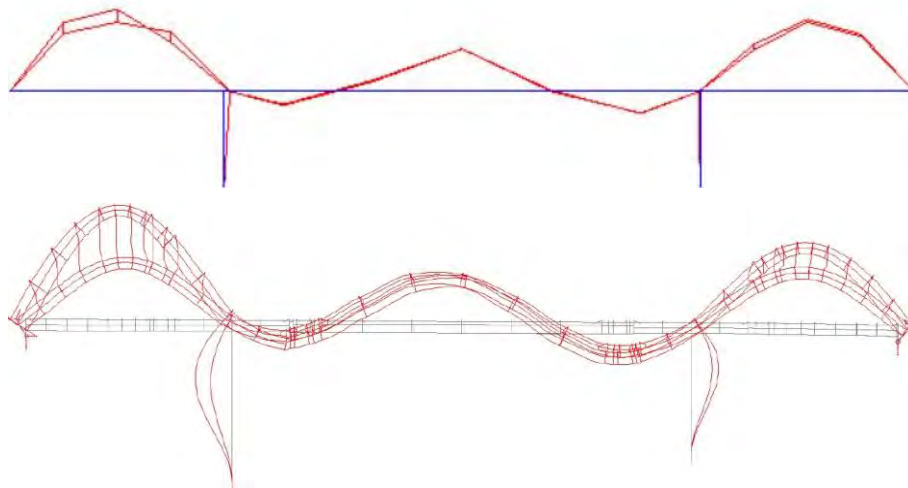


Figure 45. 3<sup>rd</sup> vertical mode

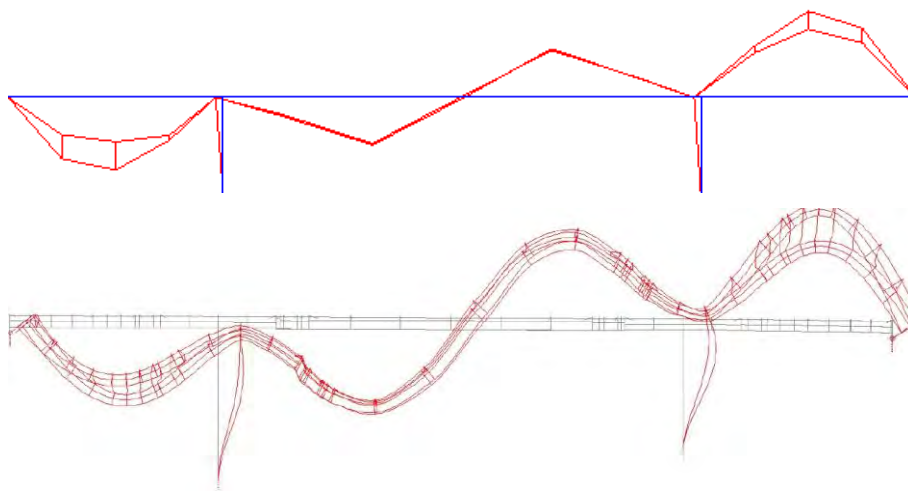


Figure 46. 4<sup>th</sup> vertical mode

Enhanced FDD Natural Frequency = 17.61 Hz - Damping Ratio = 0.7208 %

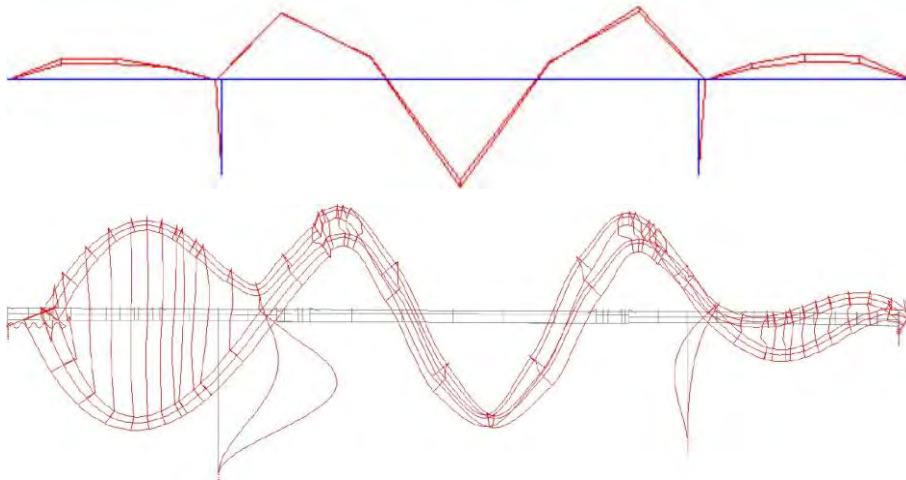


Figure 47. 5<sup>th</sup> vertical mode

Enhanced FDD Natural Frequency = 7.61 Hz - Damping Ratio = 0.8143 %

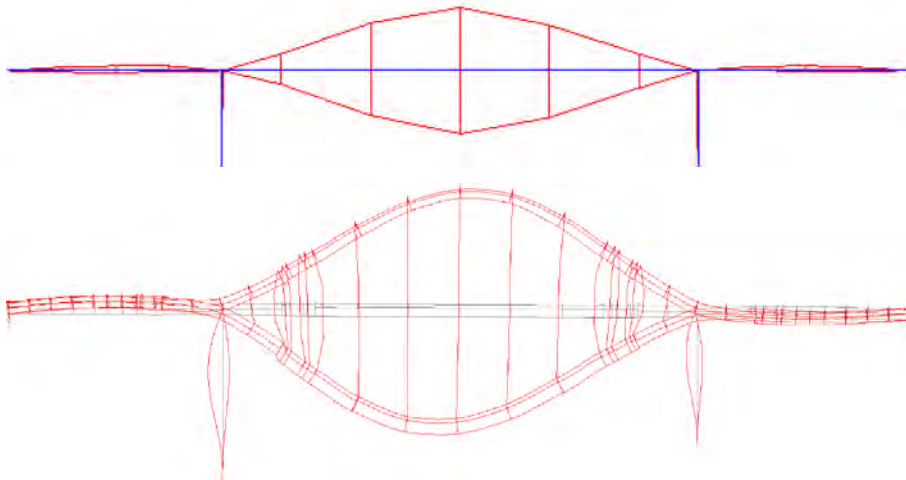


Figure 48. 1<sup>st</sup> torsional mode

Enhanced FDD Natural Frequency = 13.59 Hz - Damping Ratio = 0.6837 %

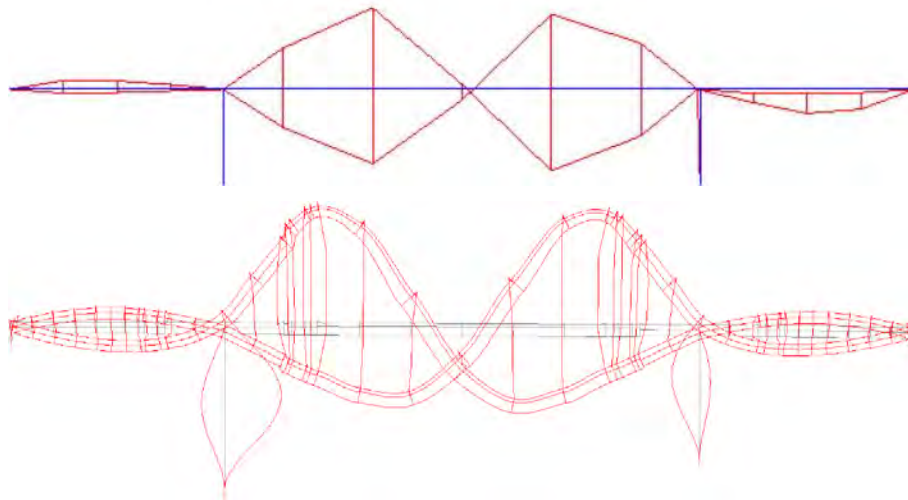


Figure 49. 2<sup>nd</sup> torsional mode

Enhanced FDD Natural Frequency = 20.24 Hz - Damping Ratio = 0.7878 %

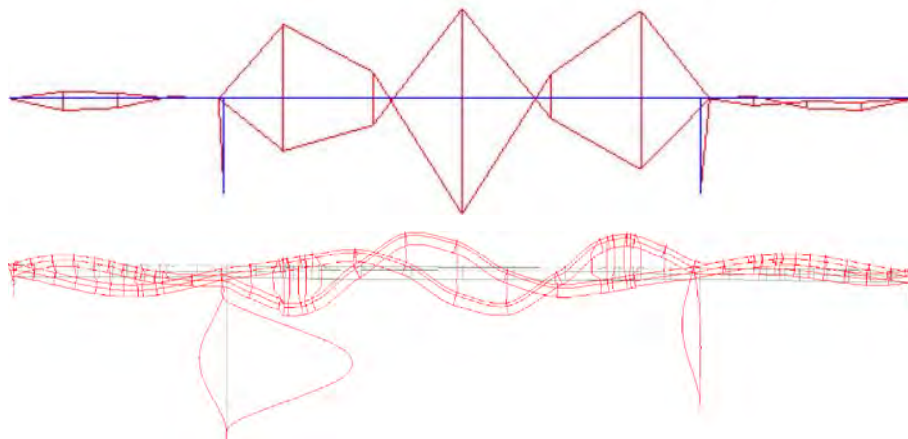


Figure 50. 3<sup>rd</sup> torsional mode

As can be seen in the figures and tables shown before, a good correlation between the measured and calculated values is evident.

## 4.5 Load test conclusions

This chapter reports the results of the load tests and the ambient vibration tests carried out by LNEC on November 11<sup>th</sup> and 12<sup>th</sup> 2021 on the overpass PS35 over the A3 Highway.

The load tests were performed with four trucks with a total weight of 997 KN. The structural behaviour was monitored by measurement of vertical displacements at the mid-span sections and rotations at the concrete-steel connections. The maximum displacement was 5.1 mm at the mid-span of the main



span. The longitudinal rotations measured simultaneously in the concrete and steel beams, near the connections, were quite similar, which means the connections behaved monolithically.

The ambient vibration tests were carried out in 3 setups without traffic interruption. The accelerations were, essentially, induced by the action of the wind and traffic below the overpass. For each setup, the acceleration was recorded for 40 min with a sampling rate of 500 Hz.

For the identification of the dynamic characteristics of the structure, the enhanced frequency domain decomposition method (EFDD) was used, which allowed the identification of 12 natural vibration modes. The frequencies of the fundamental transverse, vertical and torsional vibration modes identified were 3.948 Hz, 3.634 Hz and 7.610 Hz, respectively.

The experimental results obtained in the static load test and the dynamic tests displayed a good agreement with the analytical values computed by FE model.

In view of the above, it can be concluded that the connections between the concrete and steel deck sections behaved monolithically, demonstrating a behaviour indicative of effective continuity between both type of substructure.



## 5 Enhanced Bridge Modular Solution

### 5.1 Prototype definition

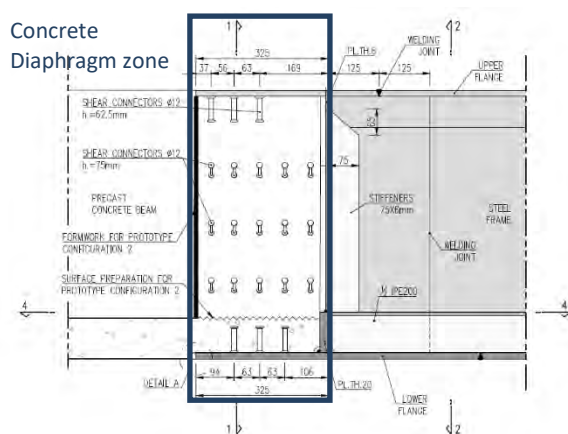
The main objective of the prototype was to test the behaviour of varying configurations and, progressively, simplified layouts of the connection piece between the steel and concrete parts of the girders. Hence, the main differences between these configurations resided in the steel-concrete connection.

Because the fabrication, transportation, and setting up of three separate prototypes would largely increase the estimated costs of the lab tests, notwithstanding the fact that it would be very demanding for the lab in terms of the time needed to conduct such an operation, the adopted procedure was to find a solution that allowed to convert one configuration into the others, hence greatly reducing the time in-between tests. This particular solution required the conversion between the three configurations to be done in a certain sequence and with careful monitoring during the execution of the tests, so as not to incur into permanent damage to the prototype that could otherwise undermine subsequent test results.

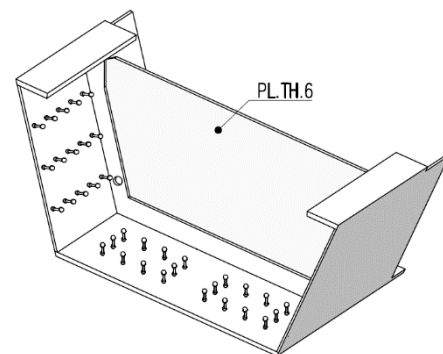
For the sake of conciseness, a brief description of each prototype configuration is given in the following paragraphs.

The first prototype configuration – **Prototype Configuration 1** – was setup with the greatest level of optimization when compared to the original design. The most prominent features of this prototype are the absence of the concrete diaphragm, the addition of steel profiles on the steel side of the connection, the absence of Perfbond connectors, and the addition of prestressing bars.

Upon execution of the prototype, the first configuration will also include the necessary features to allow its easy conversion into the other configurations. These include the concrete diaphragm reinforcements, the preparation of the concrete surface in those areas, the placement of formwork and the concreting openings in the top slab to allow pouring the concrete for the diaphragm. For the purpose of the lab tests, the prestressing forces will be applied to the model through prestressing bars instead of tendons, as initially planned. This change was justified by the fact that, with this solution, the application results much simpler. It is important to highlight that the prestressing must be applied before the casting of the upper slab / flange, in order to simulate the real connection conditions. The suppression of the Perfbond connectors also contributes greatly to this principle.

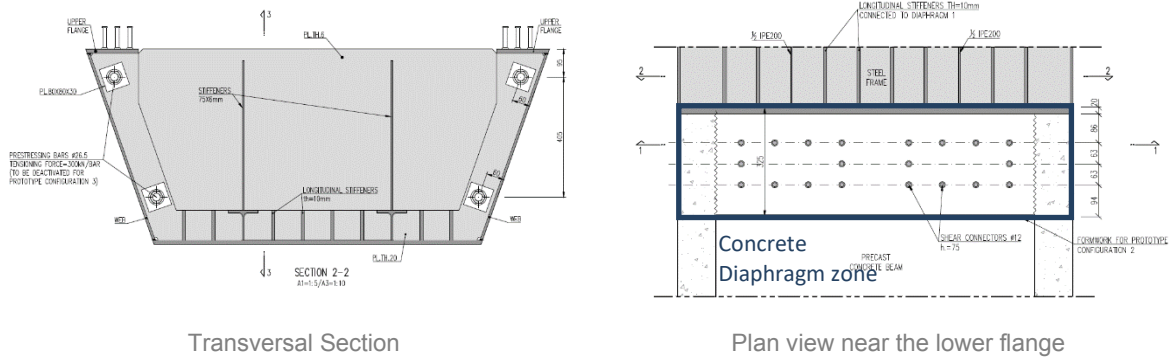


Longitudinal Section



3D perspective





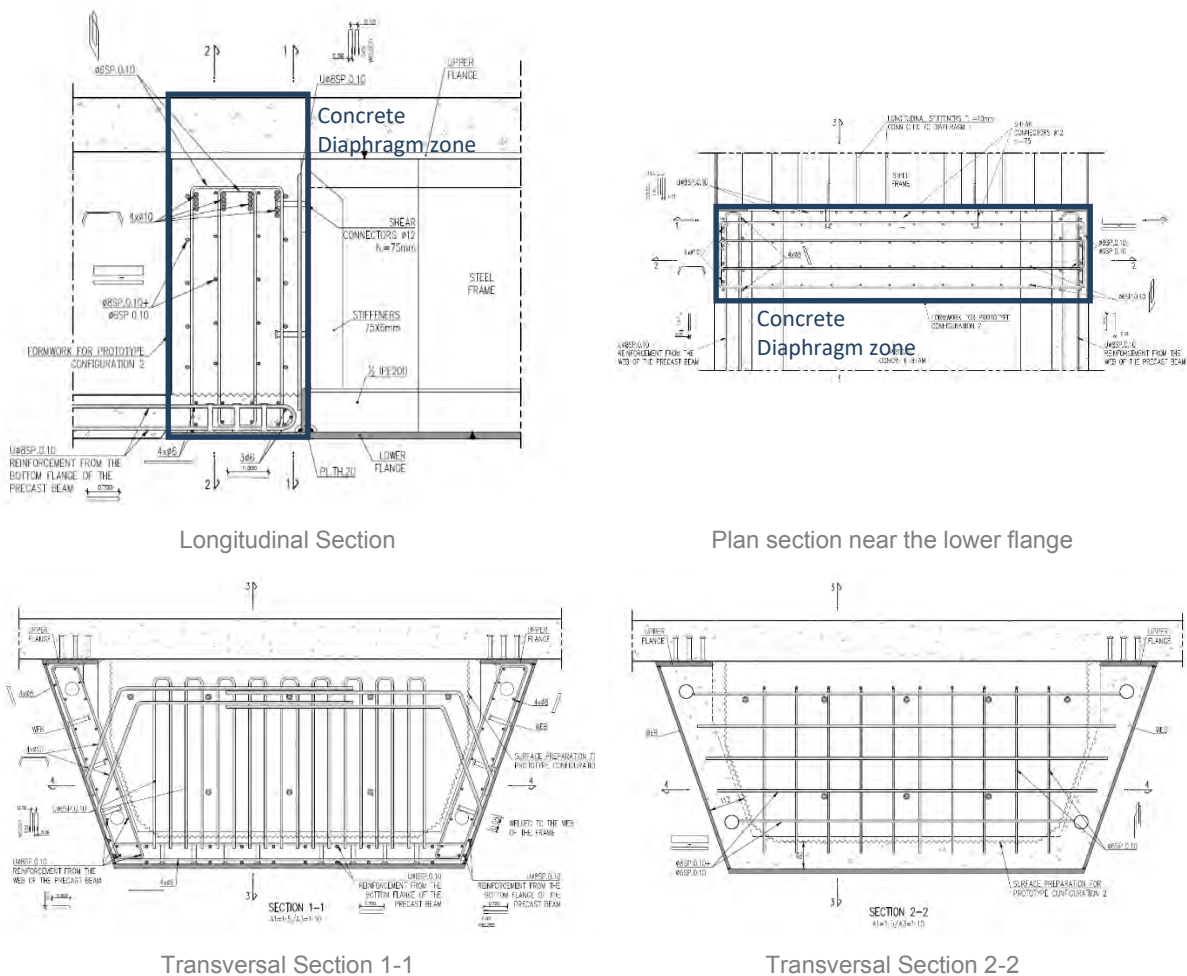
Transversal Section

Plan view near the lower flange

Figure 51. Prototype Configuration 1 overview

The prototype configurations 2 and 3 are described as follows:

**Prototype Configuration 2** – This test configuration was attained by concreting the diaphragm in the connection zone. The figures below illustrate the reinforcement bars that were assembled for Prototype Configuration 1, along with the required formwork and surface preparation at the interface, ready for concreting.



Longitudinal Section

Plan section near the lower flange

Transversal Section 1-1

Transversal Section 2-2

Figure 52. Prototype Configuration 2 overview





**Prototype Configuration 3** – The third and last test configuration was obtained by deactivating the precast concrete deck prestressing bars that were presented in both configurations, 1 and 2. The following figures provide an indication of the location of these bars.

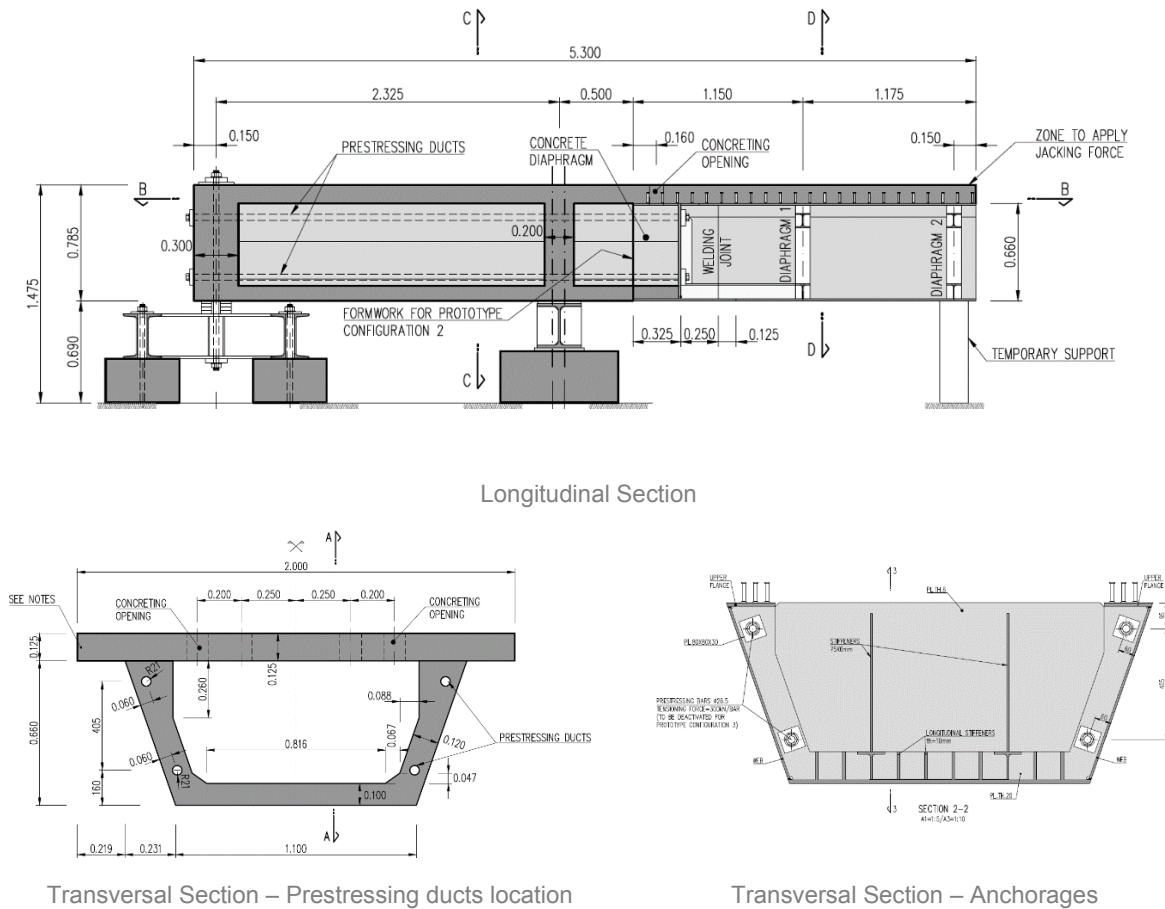


Figure 53. Prototype Configuration 3 overview

The rationale behind the definition of these prototype configurations was based on the fact that the connection between the steel and concrete is materialized through several partially redundant structural mechanisms. By evaluating the behaviour after suppressing/simplifying some of the elements, the basic requirements for the connection can be cross-checked and the solution validated.

## 5.2 Applied loads

The loading test comprises two general levels of loading corresponding to Service Loads and Ultimate Loads, as defined in the original design documents of the overpass. While the purpose, as stated before, is to optimize the design in service of a simplified fabrication and assembly, due to the fact that the connection is a critical aspect of the structure – hence its location amongst the bridge –, it is expected that the steel part of the structure remains essentially in an elastic state.

Taking into consideration the model scale (1:2), the correspondent force scale and moment scale are 1:4 and 1:8, respectively (to obtain the same stress level in the connection as for the real scale model). Hence, the loads to be applied were scaled accordingly, as summarized in the following table. The load effects presented in this table are in the connection zone and the force to be applied is located at the



tip of the prototype cantilever. The maximum force to be applied in the prototype is 550 KN. It should be noted that this force is slightly larger (about 15%) than the equivalent shear force obtained in the real scale model (Overpass PS35) for the Ultimate Limit States.

It is also important to note that the design effects obtained in the connection zone of the real scale model (Overpass PS35), and shown in the next table, are representative for similar types of overpasses since the connection is located near the pier support (zone with greatest shear forces and bending moments). Also, the 40 m span of this structure is quite typical for this kind of overpasses. Therefore, the shear and moment values defined for the real scale model are meant to be an upper bound for similar structures with similar deck widths and span arrangements.

*Table 8. Loads to apply and load effects at the connection*

Limit State	Real Scale		Prototype – Scale 1:2		
	Shear	Moment	Force to be applied	Shear	Moment
Serviceability Limit State	1 000	-4 200	250	250	-505
Ultimate Limit State	2 100	-8 300	550	550	-1 110



## 6 Design and performance of In-lab tests at LNEC

The lab tests at LNEC laboratory provided experimental data to support the analysis and enhancement of critical aspects of the solutions that are to be adopted for the construction of hybrid bridge structures on highways.

### 6.1 Objectives

The main purpose of these sets of tests is to provide experimental data on the behaviour of the steel-concrete connection piece of hybrid bridge overpasses under service and ultimate loads. Based on the fact that this hybrid design has already been tested and built for some overpasses on the A3 highway (in Portugal), this solution was proposed as a form of addressing the construction/deconstruction part of the life-cycle of the target Highways in the context of the Omicron Project.

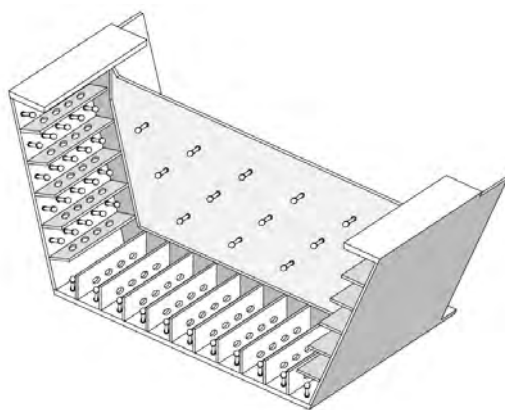


Figure 54. Connection piece (original design from PS35)

With the intent of improving several aspects of its design (after an initial design revision analysis, it was deemed that the steel-concrete connection piece might have some additional redundancy that could be used to simplify the design of the connection and the layout/process of fabrication of its constituent parts) a set of lab tests was established, comprehending the construction and testing of a prototype with three possible configurations, each with different degrees of optimization and simplification. These also include some conceptual improvements such as, for instance, a method that allows the extension of the precasting prestressing tendons through the actual connection piece, effectively mobilizing it for the purpose of improving the structural connection behaviour and material usage.

In general, the main goal of the optimization process is to simplify the design and construction of these types of solutions.

### 6.2 Description of the tests

The in-lab tests were performed at the Portuguese National Laboratory of Civil Engineer (LNEC) materials laboratory, as previously proposed, affecting a team that works closely to the responsible for the previously performed load testing of the overpass PS35 at A3 highway.



Lab tests were performed on a prototype model that constitutes a partial representation of the existing structures. Since the main focus of the tests relies on the behaviour of the connection piece, the simplest option was to model the length of the structure between the cross-section above the piers and a certain length in the central steel span, which ought to reproduce the stress distribution on the prototype once the loads are applied near the tip of the structure, equivalent to a cantilever. With this approach, equivalent values to the original design of shear force and moment are obtained in the connection.

## 6.3 Laboratory conditions

The figures below depict the basic dimension layout and support conditions for the prototype.

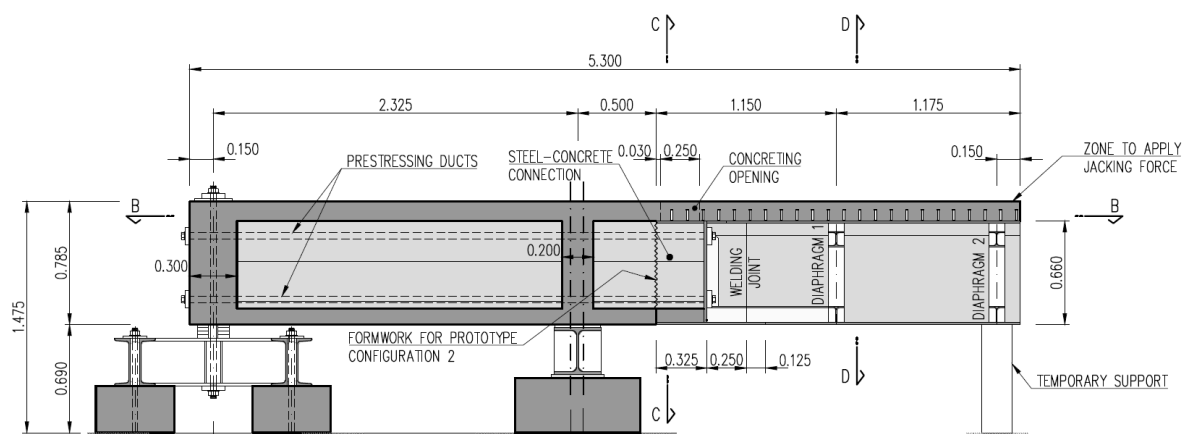


Figure 55. General layout of the prototype

One aspect of the prototype, that presents a challenge, is the fixed end at the back supports – corresponding to the sections above the piers – which require the capacity to restrain the prototype in such a way as to mobilize the fixation moment. This configures a high dependency on available LNEC’s lab conditions both for this purpose but also for the process of load application. At full scale, the objective of applying loads that reach the theoretical ultimate states results in the need for high-capacity jacks and this further increases the difficulty of materializing the fixation end of the prototype.

Furthermore, although only one of the girders was being considered for the test, even then, the size of the prototype also became an important factor in terms of its fabrication, transportation and positioning within the lab premises (for logistic reasons the prototype is to be fabricated in a different location from where it will be tested).

In conclusion, due to the constraints imposed by lab conditions, range of loading to apply and proper materialization of the structural model, a decision was made in the sense of using a scale of 1:2, which resulted in a more manageable model in terms of fabrication and transportation and easier to adapt to existing component sizes at half-size. According to the similitude theory usually used on this type of scaled model tests, this prototype scale corresponds to ratios of 1 to 4 in forces and 1 to 8 in bending moments. Therefore, the same stress range in the connection zone as the real scale overpass PS35 is achieved.

The following figures illustrate the final setup for the tests.



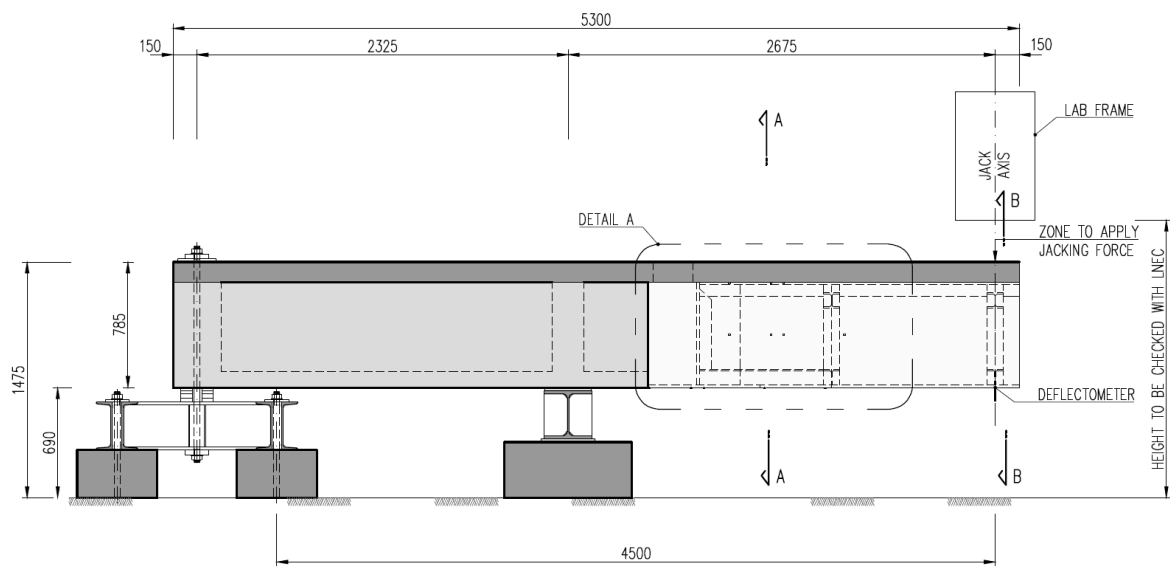


Figure 56. Prototype setup for in-lab tests

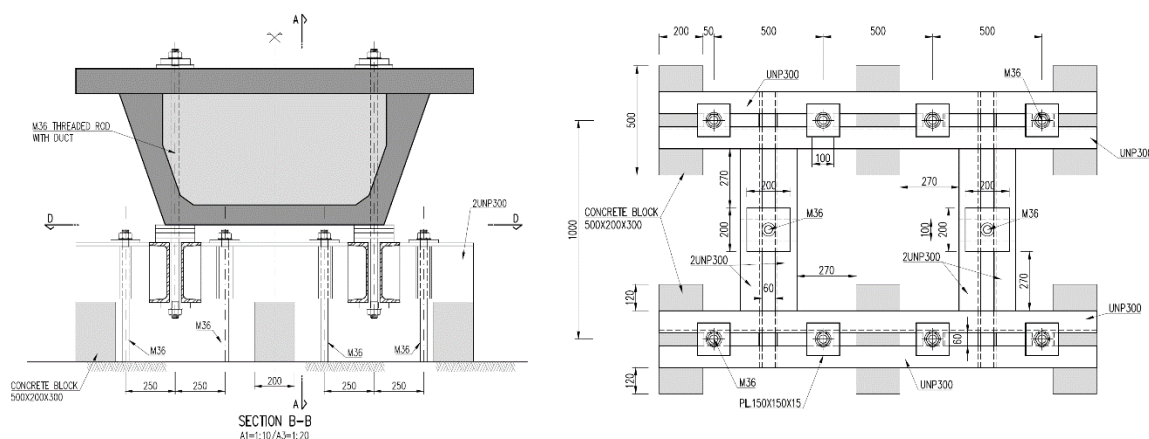


Figure 57. Rear restraining system for the prototype

It should be noted that to materialize the fixed end of the structure and properly secure it to the available lab fixation systems, a few adaptations and optimizations were required which ultimately resulted in the layout presented in the previous figures.

The prototype layout shown in the previous three figures can be divided into the following components:

- Tension support: where the tension is anchored through 8 bars that are connected to the LNEC's floor.
- Compression support.
- Reinforced concrete girder between tension and compression support (2.325 m): this length was chosen in order to control the tension forces in anchorages and the compression stress at the LNEC's floor.
- Cantilever zone, which comprises:



- Half meter of reinforced concrete girder: this length was chosen in order to have a length between the cantilever support and the steel-concrete connection similar to the height of the girder.
- Steel-concrete connection: the most important part to be studied in these experiments.
- Composite girder between the steel-concrete connection and the zone to apply the jacking force: the adopted length allows a relation between the moment and shear force equivalent to the design of PS35.

## 6.4 Fabrication, transport and installation

The prototype was produced at POTD Teixeira Duarte's Montijo facilities and then transported to LNEC's laboratory for final assembly and instrumentation setup.

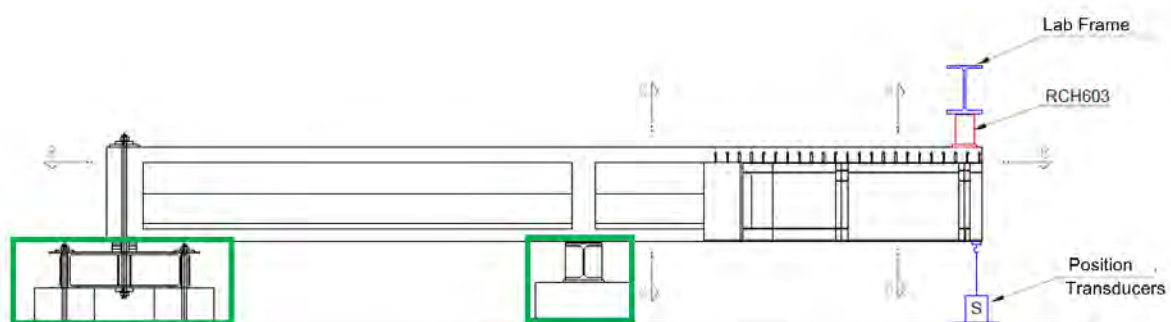
This procedure was possible because the journey from the construction site to the laboratory was short and all the necessary precautions were taken to avoid causing any damage to the prototype. However, the adaptation of the prototype between different configurations took place at LNEC's premises.

The prototype handling inside LNEC's laboratory was done by a combination of truck-mounted crane and the laboratory's bridge crane, but mainly by the former.

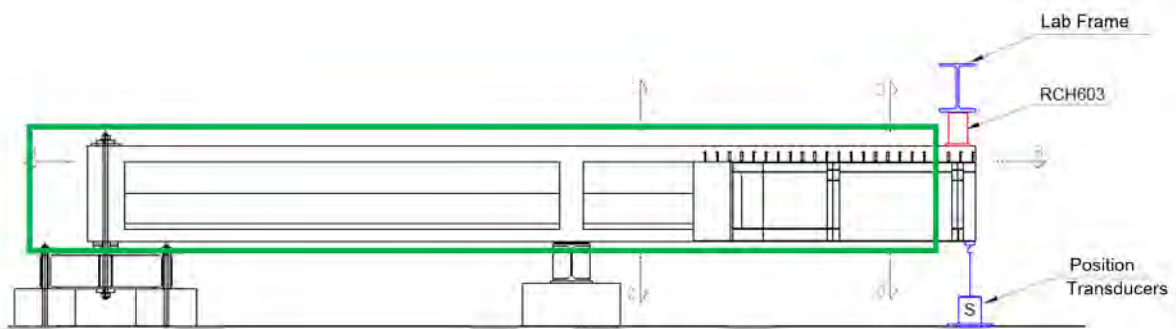
The girder/supports assembly were fixed using threaded bars directly on the floor of the LNEC's laboratory.

The installation sequence was as follows:

1. Installation of the girder/supports fixed with threaded bars, and grouting:



2. Installation of the Prototype:



3. Installation of the hydraulic equipment and sensors:

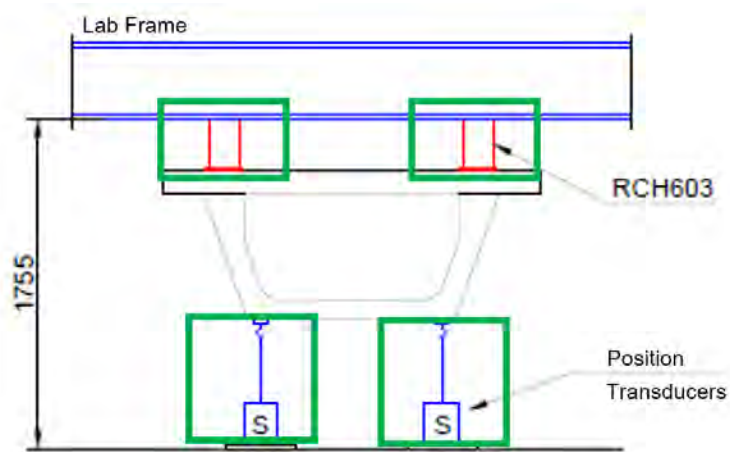
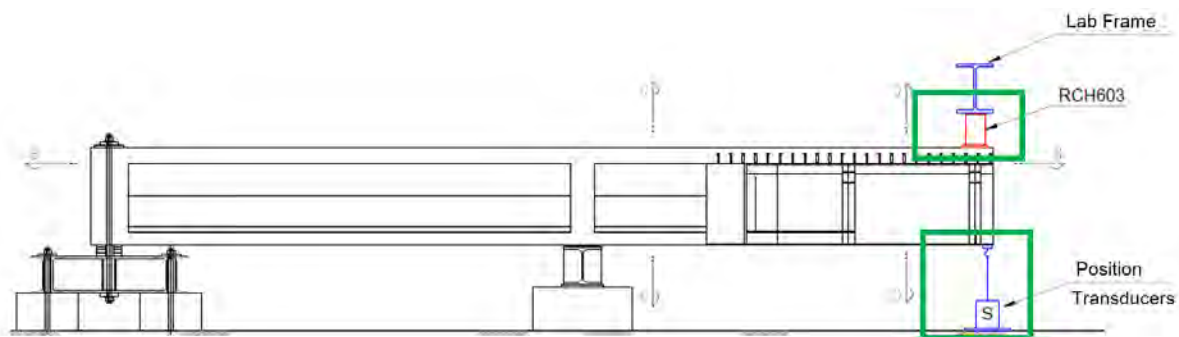


Figure 58 – Cross-section view of the laboratory assembly

## 6.5 Prototype instrumentation

To monitor the structural behaviour of the prototype, optimizing the instrumentation to be used and simultaneously obtain relevant information that allows the comparison with the results obtained in the load testing of the overpass PS35 at A3 highway, the prototype will be instrumented with:



- 5 rosette strain gauges (HBK Strain gauge series Y (RY81-6/120), rectangular rosette, 3 grids, offset 0°/45°/90°, temperature response for ferr. steel (10.8 ppm/K), nominal resistance: 120 ohms and measuring grid length: 6 mm). The goal of the rosette strain gauges is to measure strains in the three directions and, through constitutive laws, calculate shear stresses.
- 2 inclinometers (two-axis gravity inclinometers Schaevitz T233/T235 with a measurement range of  $\pm 3$  degree (Sherborne Sensors, 2002) and with a resolution of about 0.2 arcseconds.). These devices will measure longitudinal rotations in the connection zone.
- 1 deflectometer (HBM W50K, +/- 50mm inductive displacement transducer, resolution: +/- 0.001mm). These devices will measure the vertical deflection at the tip of the cantilever.
- 16 linear strain gauges (HBK strain gauges series Y (LY11-6/120), temperature response for ferr. steel (10.8 ppm/K), nominal resistance: 120 ohms and measuring grid length: 6 mm). The goal of the linear strain gauges is to measure strains in the longitudinal direction and, through constitutive laws, calculate longitudinal normal stresses.

In addition to this instrumentation, the applied force will be recorded in one channel. All data will be recorded using several multichannel automatic data acquisition units (model Spider 8 or equivalent) controlled by Catman software or equivalent, in a total of about 36 data acquisition channels.

For the quantities specified in previous chapters, the following figures illustrate the number and type of sensors required to make the measurements.

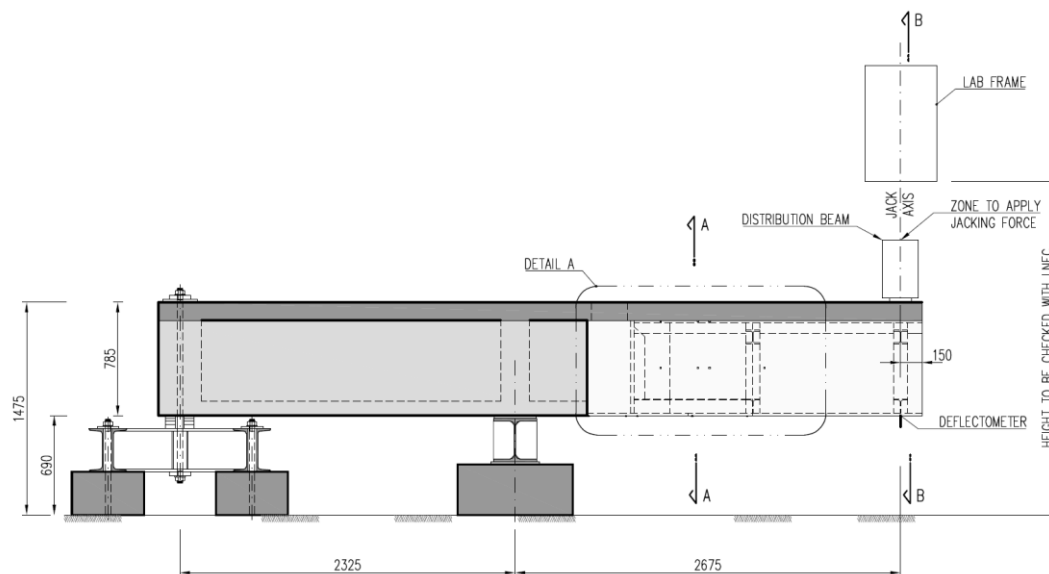


Figure 59. Instrumentation setup overview



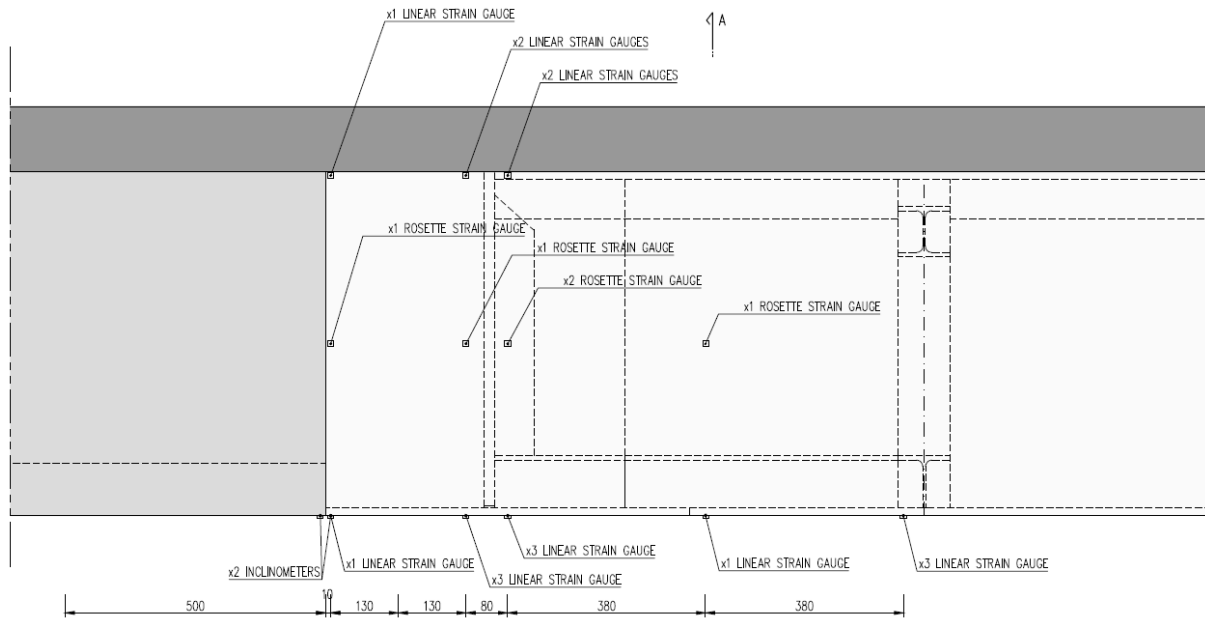


Figure 60. Detail of the instrumentation in the connection zone

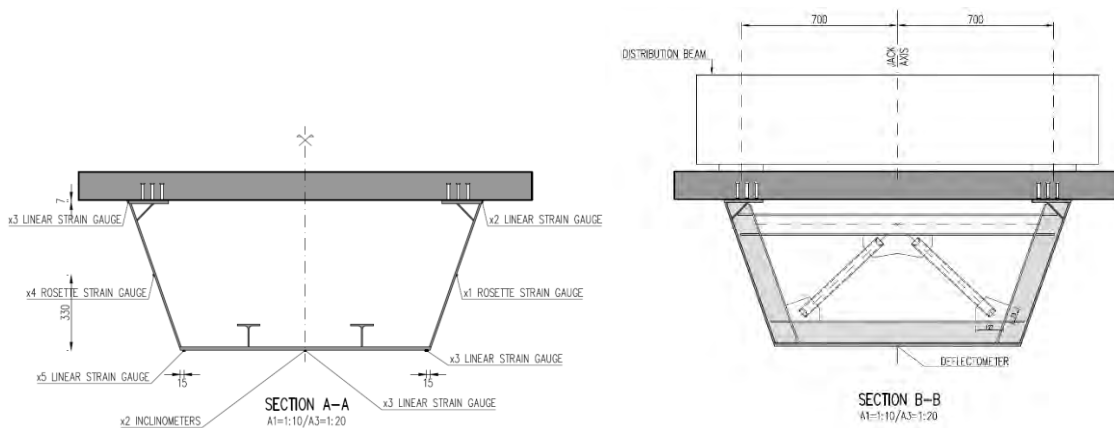


Figure 61. Location of the acquisition sensors in the cross-section

## 6.6 Expected results

The test procedure includes a few basic measurements that are intended to control the load application such as:

1. Vertical deflection at position of load application.
2. Inclination at both sides of the connection piece (similarly to the *in situ* load test).
3. Force values at the jacking equipment (via load cell).

The main results to measure during the test procedures are those that allow to survey the stress transfer from the steel parts to the concrete parts of the structure, that is, directly at the connection. This can be achieved and verified by monitoring strains in the steel flanges as well as at the midsection of the webs. Different sets of sensors can measure these quantities at both sides of the connection to investigate the different degrees of transfer.



The major goal of these measurements is to evaluate the monolithic behaviour of the three different connection layouts and compare the results between the prototype configurations. In general, the results are not easy to foresee accurately since the occurrence of some cracks in the concrete upper flange is expected with the application of forces and due to the fact that the stresses at the connection zone do not follow the Euler-Bernoulli beam theory.

The following table summarizes the expected range of the vertical deflection at position of load application. It should be noted that, due to the cracking of the upper flange, the evolution of the vertical displacement with the force increase is not expected to be linear.

Table 9. Predicted vertical deflection (mm) at position of load application

Vertical deflection	(mm)
Serviceability Limit State (250 kN)	10
Ultimate Limit State (550 kN)	35

Concerning the inclination at both sides of the connection, the expected values are not equivalent to the in situ load test since the span arrangement of PS35 is not equivalent to the lab test as the overpass PS35 has a linear elastic behaviour (uncracked concrete) for the load test performed in situ while the prototype will typically present a physically non-linear behaviour (due to cracked concrete). Hence, the main goal of these measurements is to evaluate the difference between the longitudinal rotation at the left and right side of the connection. Nevertheless, the expected values for the rotations (to be directly measured with inclinometers) are presented in the following table.

Table 10. Predicted longitudinal rotation (arc seconds) at position of load application

Longitudinal rotation	(arc seconds)
Serviceability Limit State (250 kN)	500
Ultimate Limit State (550 kN)	2000

One single hydraulic jack will be used to apply the load. The stroke of the jack should be significantly larger than the maximum vertical deflection, presented in the Table 10, since it does not take into account the lab frame deflection and a possible non monolithic behaviour of the connection.

Regarding the strain measurements, it is expected that the steel part of the structure remains in an elastic state in Bernoulli zones, which correspond to strains lower than 1.7 ‰. In the connection area, it is possible that some particular zones (due to stress peaks) are in a post-elastic behaviour. In this case, the main goal is to identify the zones where this happens and not to quantify the maximum plastic strain.

The evaluation of the results and the success of these experiments will follow the criteria presented in the following table, in order of importance.



Table 11. Criteria for the evaluation of prototype configurations

Limit State	Criterion 1	Criterion 2	Criterion 3
<b>Serviceability Limit State</b>	Visual damage evaluation. Damage level that can compromise the service life is not allowed.	Evaluation of the monolithic behaviour through the difference between the longitudinal rotation at the left and right side of the connection. The difference should be smaller than 25 arc seconds.	Strain and stress assessment. In general, stresses should be within the elastic range.
<b>Ultimate Limit State</b>	Structural failure. No failure is allowed.	Evaluation of the monolithic behaviour through the difference between the longitudinal rotation at the left and right side of the connection. The difference should be smaller than 100 arc seconds.	Visual damage evaluation. Some level of damage is allowed but it can neither induce the failure of the connection nor affect the safety of people nearby.*

\*According to EN1990, the Ultimate Limit State is related to the safety of people and/or the safety of the structure. Hence, small damages (such as concrete cracking and steel plastic deformation) that do not affect the abovementioned can be allowed.

Due to the sequence of the test procedure, including the conversion process between the different prototype configurations, special care must be taken during the execution of the tests to avoid severely damaging the prototype, which could prevent further testing and render the in-lab tests unsuccessful.

Load application shall be performed in closely monitored incremental steps. It is preferable to stop a test, even if the target force is not fully applied, in order to prevent severe damage and proceed with the other configurations. Ultimately, it will depend on the behaviour of the test prototype and the damage assessment between each step.

## 7 Prototype (scaled model) production

The prototype production was done at TDU facilities that comprises a set of technological centres focused on different services to which the construction sites recurrently call to ask assistance for their works. In time, these technological centres started to serve not only the TDU constructions but many other external clients.

Nowadays there a total of five (5) of these centres, each specializing in different areas where they intervene:

- Specialized Equipment for Construction (DEC), either heavy or light, both for use on-site or to facilitate transports (by land or sea) to the same sites.
- Framework Operational Centre (COC), with a brand new fully operational department for cutting and bending of concrete reinforcements and a consolidate knowledge on how to apply and operate pre-stressing tendons, namely through assembling, tensioning and force control.
- Metal Mechanics Fabric (MMF) with industrialized equipment for metalwork, in particular, three robotized lathes, a Computer Numerical Control (CNC) equipment to cut and drill steel pieces, a CNC for welding works and still an industrial painting stove.
- Concrete Branch Plant (CBP), with a large experience in concrete mixtures with specific compositions for special construction works, such as bridges, tunnels, geotechnical stability, among others.
- Concrete and Fillers Laboratory (CFL) that does the quality control for the CBP as well as assists any other need in terms of fillers and special mixtures, especially for geotechnical works, the mother-core activity of TDU.

All these technological centres are established in TDU Operational Yard, held in Montijo, Lisbon, Portugal, and were involved in the prototype fabrication, transportation and laboratory support works.

### 7.1 Prototype reinforced concrete part production

The prototype 1 of OMICRON project was built at POTD - Operational Centre of Teixeira Duarte, S.A in Montijo, with the support of the following departments:

- COC - Formwork and Prestressing Operational Center, which carried out the formwork.
- CPA - Reinforcements Production Center, which supplied, moulded and assembled the reinforcements.
- CPB - Concrete Production Center, which supplied the concrete.

The reinforced concrete structure of the prototype consists of a deck with a box girder section.



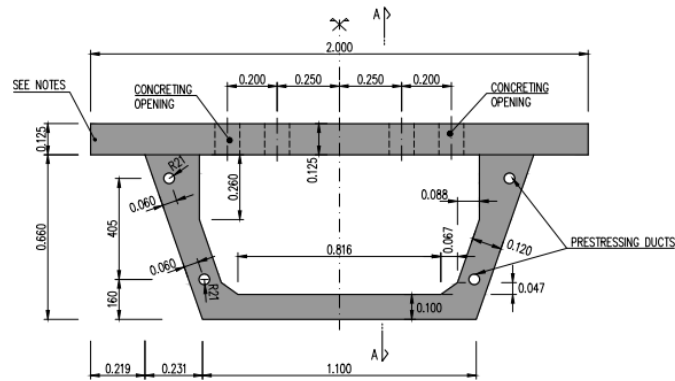


Figure 62. Concrete Box girder cross-section

The prototype was executed in 2 phases.

In the first phase, part of the reinforced concrete box girder was built consisting in the bottom slab and side walls.



Figure 63. External formwork

The second stage of prototype construction saw the addition of the upper slab of the deck.



Figure 64. Formwork and reinforcement of the upper deck slab



Figure 65. Freshly concreted upper deck slab

The reinforced concrete prototype structure was completed with the formwork removal.

## 7.2 Prototype steel structure production

The steel structure of prototype 1 of OMICRON project was built in POTD - Operational Centre of Teixeira Duarte, S.A in Montijo, with participation of CEMM - Metalworking department, based there.

The steel structure of the prototype consists of a steel (girder) section with connectors for load transfer to the reinforced concrete deck.

The supports for the feasibility of the laboratory test and the load transfer beam of the hydraulic jack were also built in steel structure.

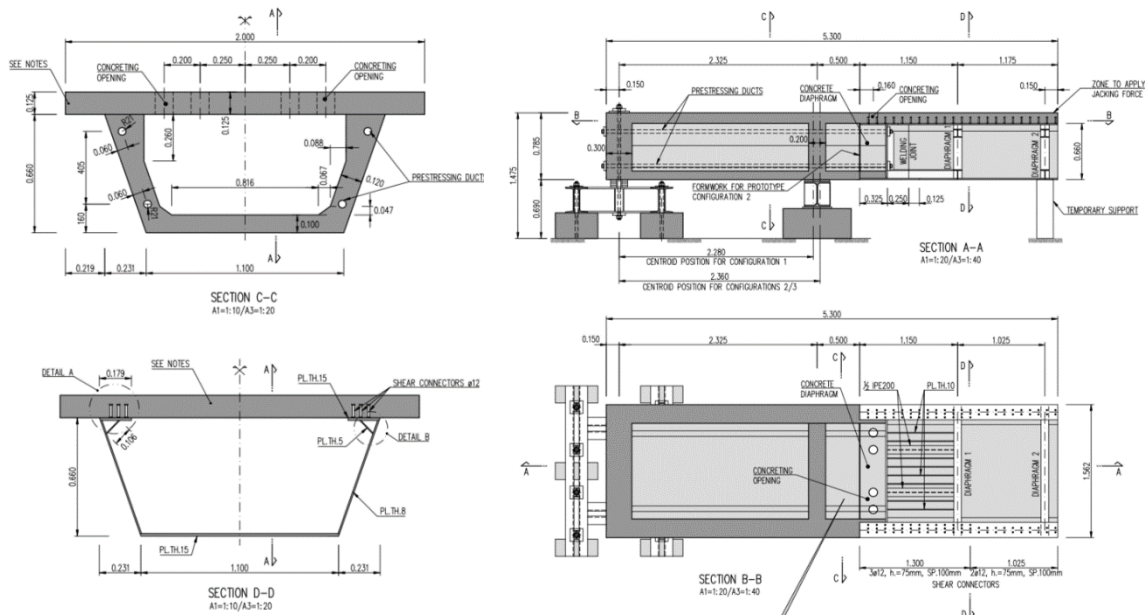


Figure 66. Construction details for the prototype

Below, some images of the structure during its construction and in the finalized phase, in the laboratory:





*Figure 67. Steel structure of the box section*



*Figure 68. Metallic structure of the box section*





Figure 69. Suspension eyebolts with tie rods



Figure 70. Support beam for the prototype of the test



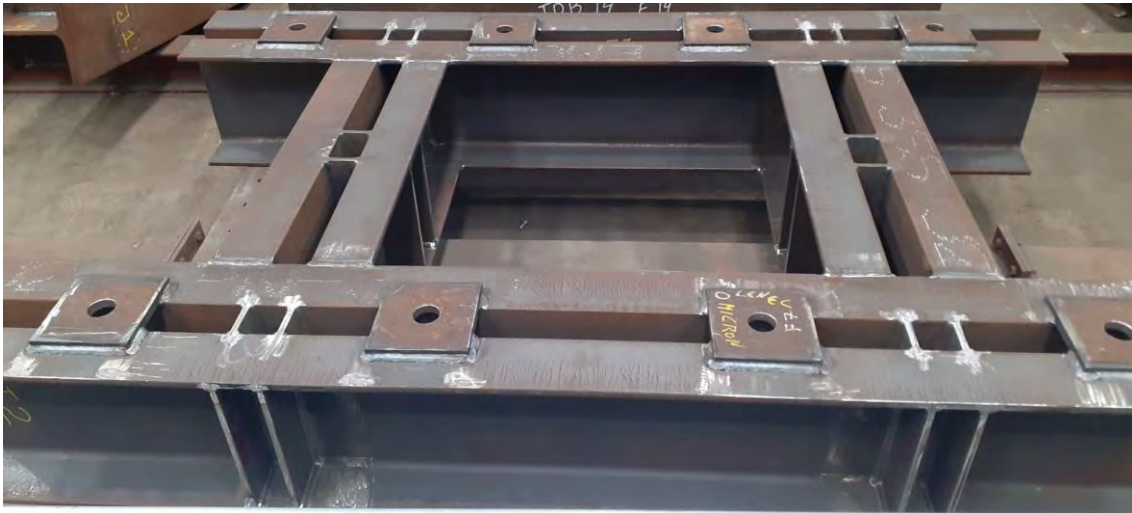


Figure 71. Rear restraining system for the prototype



Figure 72. Distribution beam for the hydraulic jack in the test

### 7.3 Prototype transportation to LNEC facilities

Transport operation of the prototype to the LNEC facilities and placing it in the test position was a delicate task because of the large weight and dimensions of the prototype and the special care that must be taken to avoid cracking or other damages that could affect the results of the laboratory tests.

Accessory devices were placed to allow the mobilization of the prototype. The prototype was weighed to ensure that the load was under the load capacity of the laboratory crane.



*Figure 73 and Figure 74. Installing the eyebolts for prototype mobilization and weighing*

The placement of the prototype in LNEC's facilities was done with the help of a service for special transportations.



*Figure 75. Prototype transportation*





*Figure 76. Prestressing the prototype in the laboratory*

After the conclusion of the laboratory tests, the prototype was transported back to the TD facilities in Montijo.



*Figure 77. Prototype stored in the POTD*

## 8 In-lab tests

With the arrival of the prototype at the LNEC's premises, which took place on the 20<sup>th</sup> September 2022, the final tasks of assembling the measurement instrumentation, systems setup and equipment calibration were able to start.

### 8.1 Instrumentation

Figures below shown the instrumentation and systems setup and calibration.



Figure 78. Instrumentation assembly at LNEC's premises

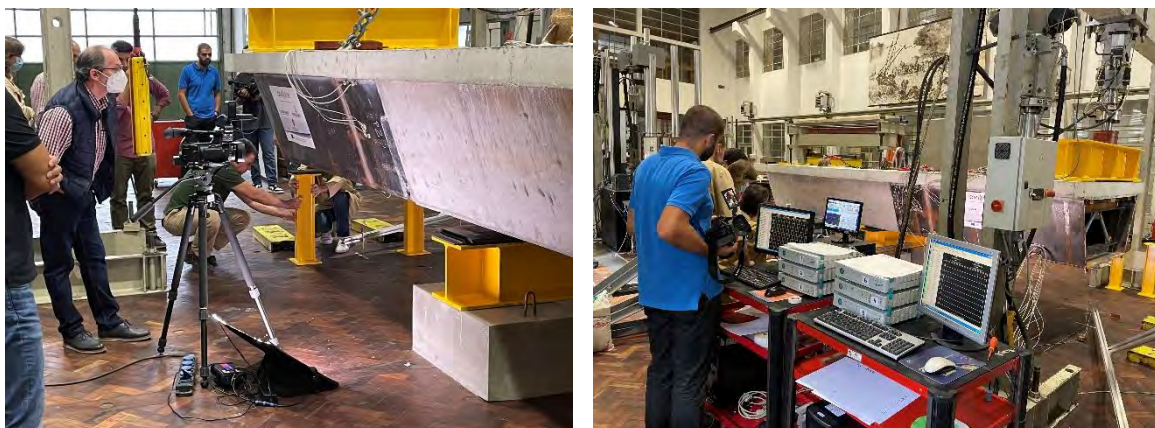


Figure 79. Instrumentation, control systems setup and calibration





Figure 80. Instrumentation: strain gauges and clinometers

## 8.2 Laboratory tests

The tests were performed, for each proposed configuration, on the 19th, 25th and 27th October 2022.



Figure 81. Laboratory – Prototype being tested – front view



Figure 82. Laboratory – another view of the prototype during the tests



Figure 83. Laboratory – Prototype being tested – back view

### 8.3 Preliminary results

Following the realization of the in-lab tests, the resulting data can be shown in this section in the form of graphs, such as Load-Displacement charts as well as rotation measurements in tabular form. However, a full formal results analysis will be presented in the next deliverable, D4.3. The laboratory will provide the relevant data in a post-processed form, from which the subsequent analysis will be finalised.



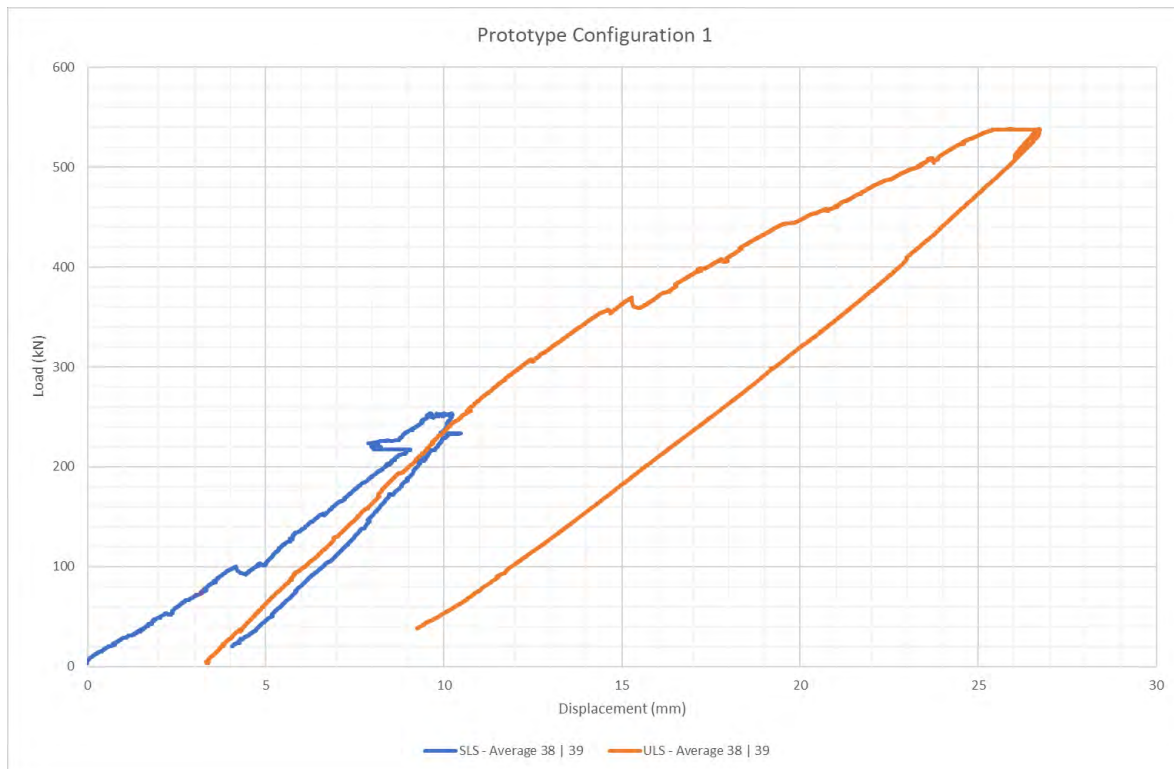


Figure 84. Load-displacement curve for the Configuration 1

As it can be seen from the previous figure, the SLS load level of 250 kN was successfully reached and, after an initial full unload process, the prototype was gradually subjected to an incremental force up to ULS level of 550 kN.

The ascending branch of the curves, that is the loading part of the curves on the first Configuration, is noticeably more “jagged” and irregular than in the subsequent configurations (see next figure). This is probably due to the test setup (supports, lab frames, the prototype and its restraining systems) being slightly adjusted to the load action and also due to the occurrence of some cracking.

It should be noted that during the first test the concrete blocks supporting the prototype exhibited cracking due to the fact that they were not properly reinforced and, along with that, some displacement (less than 5 mm) was observed at the plates of the restraining system. Also, the convex nature of the first ascending branch (particularly when the load was taken to ULS levels) is somewhat representative of and coherent with these behaviours.

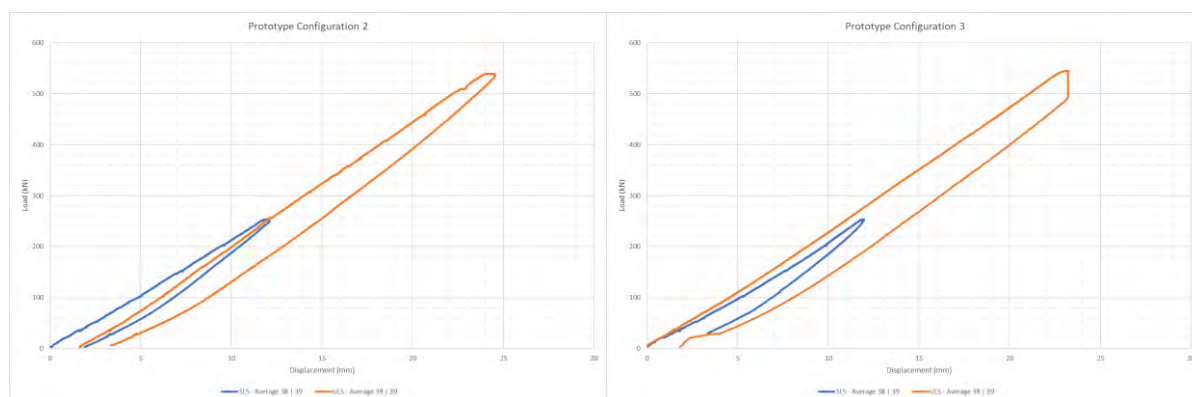


Figure 85. Load-displacement curves for Configurations 2 & 3

In a similar way, the descending branch during the unloading process, follows an almost-linear path, minus the irregularities mentioned before, albeit in a somewhat concave shape. In all subsequent configuration tests, the loading and unloading paths follow this shape, meaning that the stiffness and overall state of the prototype were preserved for these tests while attaining the target load levels, as intended. It should also be relevant to refer that, for these tests, the concrete blocks were replaced by steel blocks and the gap in the restraining system bars was eliminated which may also have contributed to the more stable shape that was obtained in the load-displacement charts.

Concerning the structural behaviour, the first evaluation that could be made is to compare the measured rotations at the connection in the three tests against the predictions made during the design stage.

Table 12. Summary table with some preliminary results for the rotations at the connection (LNEC)

Prototype	Configuration 1		Configuration 2		Configuration 3	
	SLS	ULS	SLS	ULS	SLS	ULS
Limit State						
Max. Load (kN)	253.33	538.27	245.06	539.34	253.64	544.65
Max. Long. Rotation - Concrete (40) (arc seconds)	507.17	1469.66	638.50	1403.14	653.18	1411.78
Max. Long. Rotation - Steel (42) (arc seconds)	512.35	1487.81	577.15	1270.08	593.57	1265.76
Max. Long. Difference (40 42) (arc seconds)	7.78	19.01	62.21	133.92	60.48	146.88
Foreseen longitudinal rotation at the connection (arc seconds) *	500	2000	500	2000	500	2000
SLS Criterion 2 for the evaluation of prototype configurations *	< 25	-	< 25	-	< 25	-
ULS Criterion 2 for the evaluation of prototype configurations *	-	< 100	-	< 100	-	< 100



Prototype	Configuration 1		Configuration 2		Configuration 3	
Limit State	SLS	ULS	SLS	ULS	SLS	ULS
Max. Trans. Rotation - Concrete (41) (arc seconds)	-222.05	-362.02	-197.86	-182.30	-135.65	-140.83
Max. Trans. Rotation - Steel (43) (arc seconds)	-262.66	-490.75	-240.19	-270.43	-188.35	-251.42
Max. Trans. Difference (43   41) (arc seconds)	41.47	137.38	54.43	123.55	53.57	120.96

\* Calculations by Armando Rito and Teixeira Duarte (2022). WP4, TD1 Task T4.1.2, Laboratory Tests.

As it can be seen from the results in the previous table, the absolute rotation values strongly agree with the predictions, in particular for the SLS level. For the “Ultimate Load” of 550 kN, the results are not as much “on spot”, but the measured value is lower than the prediction which is a result that was expected, meaning that the non-linear effects were slightly overestimated (a conservative approach was taken for these predictions). Both in SLS and ULS the rotation difference measured by the two sets of clinometers was small and always less than the established threshold (as set in the design stage), which is a satisfying result.

For the configuration 2 and 3 tests, there was a slight increase of the rotations for both the absolute value and maximum difference between the sets. This occurred for both SLS and ULS levels and is somewhat coherent with the resulting load-displacement curve shapes mentioned before.



## 9 Conclusions and next steps

### 9.1 Conclusions

The objective of use case 4 of OMICRON is the development of enhanced modular solutions for pre-manufactured overpass bridges. The idea is to minimize the construction site operations, especially the works that take place above the traffic lanes, so as to keep them under circulation.

The main goal in this respect is to review and enhance the design of the connection elements in hybrid steel-concrete bridges, in order to ensure their robustness performance-wise and safety-wise. In this respect, the project aims to provide a methodology to minimize the adjustments required and to make a more general use of this solution, for instance, in scenarios with different span arrangements.

The progress of this use case has resulted in:

- An on-site monitoring campaign comprising load tests on an existing structure.
- Lab tests on prototype models.
- Structural analyses with analytical models to develop this improved design methodology.

The on-site monitoring campaign has provided insights on previous, similar designs in order to propose an enhanced simplified solution. At the same time, the in-lab tests have provided information on the three design prototypes, verifying the suitability of all of them. In the next stages of the project, the in-lab tests will be fully analysed, and a virtual demonstrator of the solution will be showcased, as presented in the next sub-section.

### 9.2 Next steps

#### 9.2.1 In-lab tests result analysis

The test results are still being treated and analysed by Armando Rito, Teixeira Duarte and LNEC. While being preliminary, the presented charts and values show a good performance of all the test solutions. The first task of the next stage is to present a detailed and thorough analysis of the results in light of the project objectives.

#### 9.2.2 Virtual demonstrator

The remaining tasks of the final stage are centred on the production of a virtual demonstrator for an enhanced hybrid bridge solution using BIM methodologies.

For this objective two activities are planned:

- The production of a parametric BIM model which will be able to provide a material and cost estimate for a generic set of highway hybrid overpass solutions, given some base parameters such as the number of overpass crossings, highway profile width, overpasses widths. The overpass model would be automatically adjusted to these boundary conditions.
- The realization of a digital and animated simulation of the erection process involving the developed enhanced hybrid solutions for an example use case. This could be used to showcase the differences and gains against other solutions such as traditional reinforced concrete, precast or steel-concrete composite bridges.



## 10 References

Armando Rito. (2012). *Steel-concrete connection concept*.

Cabral, Bispo, & Rito. (2012). *Hibrid design for bridge overpasses. The PS35 bridge*.

SVS. (2005). *ARTEMIS Extractor Software*.

